Published in final edited form as:
J Geophys Res Atmos. 2021 October 27; 126(20): . doi:10.1029/2021jd034916.

Biomass Burning Over the United States East Coast and Western North Atlantic Ocean: Implications for Clouds and Air Quality

Ali Hossein Mardi[1], **Hossein Dadashazar**[1], **David Painemal**[2,3], **Taylor Shingler**[3], **Shane T. Seaman**[3], **Marta A. Fenn**[2,3], **Chris A. Hostetler**[3], **Armin Sorooshian**[1,4]

[1]Department of Chemical and Environmental Engineering, University of Arizona, Tucson, AZ, USA

[2]Science Systems and Applications, Inc., Hampton, VA, USA

[3]NASA Langley Research Center, Hampton, VA, USA

[4]Department of Hydrology and Atmospheric Sciences, University of Arizona, Tucson, AZ, USA

Abstract

Biomass burning (BB) aerosol events were characterized over the U.S. East Coast and Bermuda over the western North Atlantic Ocean (WNAO) between 2005 and 2018 using a combination of ground-based observations, satellite data, and model outputs. Days with BB influence in an atmospheric column (BB days) were identified using criteria biased toward larger fire events based on anomalously high AERONET aerosol optical depth (AOD) and MERRA-2 black carbon (BC) column density. BB days are present year-round with more in June–August (JJA) over the northern part of the East Coast, in contrast to more frequent events in March–May (MAM) over the southeast U.S. and Bermuda. BB source regions in MAM are southern Mexico and by the Yucatan, Central America, and the southeast U.S. JJA source regions are western parts of North America. Less than half of the BB days coincide with anomalously high $PM_{2.5}$ levels in the surface layer, according to data from 14 IMPROVE sites over the East Coast. Profiles of aerosol extinction suggest that BB particles can be found in the boundary layer and into the upper troposphere with the potential to interact with clouds. Higher cloud drop number concentration and lower drop effective radius are observed during BB days. In addition, lower liquid water path is found during these days, especially when BB particles are present in the boundary layer. While patterns are

Correspondence to: A. Sorooshian, armin@email.arizona.edu.
Author Contributions:
Conceptualization: Ali Hossein Mardi, Armin Sorooshian
Formal analysis: Ali Hossein Mardi, Hossein Dadashazar, Marta A. Fenn
Funding acquisition: Armin Sorooshian
Investigation: Ali Hossein Mardi, Hossein Dadashazar, Taylor Shingler, Shane T. Seaman, Chris A. Hostetler
Methodology: Ali Hossein Mardi, David Painemal
Project Administration: Armin Sorooshian
Resources: Armin Sorooshian
Supervision: Armin Sorooshian
Writing – original draft: Ali Hossein Mardi
Writing – review & editing: Hossein Dadashazar, David Painemal, Taylor Shingler, Shane T. Seaman, Marta A. Fenn, Chris A. Hostetler, Armin Sorooshian

Supporting Information:
Supporting Information may be found in the online version of this article.

suggestive of cloud-BB aerosol interactions over the East Coast and the WNAO, additional studies are needed for confirmation.

1. Introduction

Wildfires, agricultural burning, and other forms of biofuel consumption represent a significant source of gaseous and particulate emissions that can be transported far distances (Akagi et al., 2011; Andreae, 2019; Cook et al., 2007; Crutzen & Andreae, 1990; Heald et al., 2006; Park et al., 2007; Val Martin et al., 2013) impacting surface air quality, cloud formation and the hydrological cycle, and climate (Ackerman et al., 2000; Hobbs et al., 1997; Johnson et al., 2004; Malm et al., 2004; Mao et al., 2011; Martin et al., 2006; Park et al., 2007; Penner et al., 1992). Biomass burning (BB) research has intensified in recent years targeting the western United States (U.S.) owing to the increased frequency and intensity of wildfires as a result of climate change, land management, and fire suppression policies (Abatzoglou & Williams, 2016; Barbero et al., 2015; Schmidt, 2002; Westerling & Swetnam, 2003). In the U.S., BB accounts for up to 25% of primary $PM_{2.5}$ (particulate matter with aerodynamic diameter ≤2.5 μm) emissions annually (U.S. EPA, 2014).

While the western U.S. has been studied extensively in connection to major summertime events, field campaigns such as the International Consortium for Atmospheric Research on Transport and Transformation (ICARTT) (Fehsenfeld et al., 2006), Two-Column Aerosol Project (TCAP) (Berg et al., 2016; Müller et al., 2014), the Wintertime INvestigation of Transport, Emissions, and Reactivity (WINTER) (Schroder et al., 2018; Sullivan et al., 2019), and the Fire Influence on Regional to Global Environments and Air Quality (FIREX-AQ) (Junghenn Noyes et al., 2020) showed that BB emissions are an important pollution source over the eastern U.S. ICARTT measurements revealed the distinct influence from wildfires over the boreal forests of western Canada and Alaska on the eastern U.S. and western North Atlantic Ocean (WNAO; defined here as the marine region bounded by 25°–50°N and 60°–85°W) (Clarke et al., 2007; de Gouw et al., 2006; Heald et al., 2006; Peltier et al., 2007; Sullivan et al., 2006; Thornhill et al., 2008; Warneke et al., 2006). As one quantitative example, as much as 30% of the observed enhancement in carbon monoxide (CO) over the New England area during measurement periods in summer of 2004 was from fires from Alaska and Canada, whereas the rest was from anthropogenic emissions (Warneke et al., 2006). During the wintertime, organic aerosol from BB accounts for a third of the boundary layer submicrometer organic aerosol mass over the northeast U.S. (Schroder et al., 2018), with an important fraction derived from residential wood burning (Schroder et al., 2018; Sullivan et al., 2019). Kaulfus et al. (2017) reported that there is frequent smoke occurrence over the southeastern U.S. due to both local burning and long-range transport assisted in part from anticyclonic circulation bringing Central American fire emissions toward the southeastern U.S.

In contrast to the eastern U.S., the outflow of BB emissions over the WNAO has been studied less, partly owing to the difficulty of conducting measurements without surface stations (Sorooshian et al., 2020). The PICO-NARE mountaintop site in the Azores has been one location over the eastern North Atlantic showing clear evidence of transported BB

emissions from North America (Honrath et al., 2004; Val Martín et al., 2006; Zhang et al., 2017). Mead et al. (2013) speculated based on aerosol composition data that BB emissions can reach the island of Bermuda, which was more recently confirmed by Aldhaif et al. (2021).

Remaining knowledge gaps include the spatial, vertical, and temporal characteristics of BB air masses over the East Coast and WNAO, which is important for the understanding of vertical heating rates, thermodynamic stability in the troposphere, and potential interactions with clouds. Given the reduced levels of anthropogenic pollution in the U.S. linked to stricter regulations in recent decades (e.g., Hand et al., 2012; Jongeward et al., 2016), it is expected that the relative influence of BB aerosol particles will increase over the U.S. East Coast (Kaulfus et al., 2017) and the WNAO, with uncertain effects on air quality, clouds, and radiative forcing.

This work characterizes the spatiotemporal and vertical profile of BB aerosol particles, in addition to their potential interactions with clouds, over the U.S. East Coast and the WNAO region. We analyze the seasonal and interannual patterns of BB air masses over four different sub-regions of the U.S. East Coast in addition to a sub-region surrounding Bermuda, which has been long the subject of many studies examining offshore pollution transport from North America (e.g., Aldhaif et al., 2021; Chen & Duce, 1983; Dickerson et al., 1995; S. L. Huang et al., 1999; Milne et al., 2000). We subsequently examine spatial maps based on black carbon (BC) column density to identify transport corridors and source regions contributing to BB pollution over each sub-domain as a function of season. The impact of BB on surface air quality along the entire U.S. East Coast is assessed using surface aerosol data. In addition, vertical characteristics of BB air masses are analyzed with the use of lidar retrievals from both space and airborne platforms. Finally, relationships between BB particles and clouds are explored using a combination of data sets.

2. Experimental Methods

2.1. Study Region and Time Period

The study region comprises five sub-domains (Figure 1): four over the East Coast (NE = northeast U.S., MA-N = northern mid-Atlantic states, MA-S = southern mid-Atlantic states, SE = southeast U.S.) and a fifth centered over Bermuda. The latter is chosen as it is the only area over the remote WNAO from which surface-based data are available over a long-term period, whereas the former four collectively cover most of the East Coast, are of relatively similar areas, and offer comparable data availability. The time period evaluated is from January 1, 2005 through December 31, 2018, chosen based on co-availability of data sets analyzed in this work. A summary of data products used (e.g., product name, spatial and temporal resolution, download address, and references) can be found in Table S1 in Supporting Information S1.

2.2. Parameters Used for BB Detection

Several parameters were evaluated to develop a method for the detection of BB on a given day (i.e., “BB days”). BB days are defined as having smoke influence somewhere in the

tropospheric column and not necessarily in the surface layer. Section S1 in Supporting Information S1, including Tables S2–S5 and Figure S1 in Supporting Information S1, summarizes how we arrived at our final criteria, by comparing multiple data sets with the goal of selecting parameters that consistently detect smoke events. Here, we rely on aerosol optical depth (AOD) at 500 nm from the AErosol RObotic NETwork (AERONET) (Holben et al., 1998) and the NASA Modern-Era Retrospective analysis for Research and Applications version 2 (MERRA-2; Gelaro et al., 2017) BC column density product (hereafter referred to as BC). More details about AERONET and MERRA-2 are provided in Section S1 in Supporting Information S1. Briefly, AERONET is a ground-based aerosol remote sensing network allowing for determination of AOD among other optical quantities. MERRA-2 is a long-term atmospheric reanalysis including an aerosol transport model and an assimilation module to provide simulations constrained with observations. Either of the following conditions had to be satisfied to qualify as a BB day: (a) both parameters (i.e., AOD and BC) exhibited a deseasonalized sub-domain averaged value exceeding the 90th percentile for that respective parameter on a single day; or (b) either one of the two parameters was above the 90th percentile for 2 consecutive days. This methodology mainly detects large-scale BB events and may miss smaller ones that are more local in nature. While methodological changes would possibly affect the analysis, consistency across different data sets lends confidence to the adequacy of our methodology.

2.3. Surface $PM_{2.5}$ Mass and Composition

Although this study focuses on BB influence in the atmospheric column, it is still of interest to additionally assess the impact of BB emissions on surface air quality for the U.S. East Coast sub-domains. To do so, aerosol monitoring stations (shown in Figure 1) were selected from the Interagency Monitoring of Protected Visual Environments (IMPROVE) network (Malm et al., 1994). IMPROVE data are not available for Bermuda. We use IMPROVE stations providing data for the time period of interest between January 1, 2005 and December 31, 2018. Details associated with each IMPROVE station are presented in Table S6 in Supporting Information S1.

Aerosol collection is conducted every third day for 24 hr. Total $PM_{2.5}$ and PM_{10} mass concentrations are determined gravimetrically. Speciated data correspond to the $PM_{2.5}$ fraction and are based on either ion chromatography analysis (water-soluble ions), X-ray fluorescence and particle-induced X-ray emission (elements), or thermal optical analysis (OC and elemental carbon [EC]) (Chow et al., 2007, 2015; Solomon et al., 2014). Because of documented enhancements in BB air masses (e.g., Reid et al., 2005; Schlosser et al., 2017), we focus on data for $PM_{2.5}$, PM_{10}, EC, OC, SO_4^{2-}, and K.

The analysis presented in Table S13 in Supporting Information S1 and referred to in Section 3.5 depended on identifying BB days with anomalously high $PM_{2.5}$ concentrations. To accomplish this categorization of days, $PM_{2.5}$ data were deseasonalized by subtracting the corresponding 30-day moving average values, similar to parameters described in Section S1 in Supporting Information S1. Values are considered anomalously high when the deseasonalized values exceed the 90th percentile of every measurement during the study period. $PM_{2.5}$ is chosen for this calculation as it represents arguably the most important

parameter for air quality monitoring purposes and was usually one of the most enhanced IMPROVE parameters on BB days. Other than using deseasonalized values for identification of special days referred to as BB + $PM_{2.5}$ days in Table S13 in Supporting Information S1 and Section 3.5, discussion of IMPROVE mass concentrations throughout this work is based on the raw mass concentration data.

2.4. Aerosol Extinction Profiles

All data used in this work can be found at the following sites: NASA Atmospheric Infrared Sounder (AIRS): http://dx.doi.org/10.5067/AQUA/AIRS/DATA202. NASA Ozone Monitoring Instrument (OMI): http://dx.doi.org/10.5067/MEASURES/AER/DATA203. NASA Modern-Era Retrospective analysis for Research and Applications, Version 2 (MERRA-2): http://dx.doi.org/10.5067/KLICLTZ8EM9D. NASA AErosol RObotic NETwork (AERONET): https://aeronet.gsfc.nasa.gov/new_web/download_all_v3_aod.html. Interagency Monitoring of Protected Visual Environments (IMPROVE): http://views.cira.colostate.edu/fed/SiteBrowser/Default.aspx. ACTIVATE aircraft data: https://www-air.larc.nasa.gov/missions/activate/index.html. NASA Cloud-Aerosol Lidar with Orthogonal Polarization (CALIOP): https://subset.larc.nasa.gov/calipso. NASA CERES-MODIS: https://ceres.larc.nasa.gov/data/.

2.5. Airborne Case Study Flight

Data are shown from a case flight of the Aerosol Cloud meTeorology Interactions oVer the western ATlantic Experiment (ACTIVATE) to represent vertical characteristics of BB aerosol particles over the WNAO. Research Flight 28 on August 26, 2020 was comprised of a joint flight with the HU-25 Falcon and UC-12 King Air based out of NASA Langley Research Center (37.1°N, 76.4°W). The campaign concept and platform payloads are summarized elsewhere (Sorooshian et al., 2019). Briefly, the two planes fly in a coordinated way. The Falcon flies in the boundary layer for in situ sampling of gases, aerosols, clouds, and meteorological parameters. The King Air flies above the boundary layer and relies on dropsondes for measuring weather parameters, in addition to remote sensing instruments observing cloud and aerosol particles. This study specifically makes use of the King Air's nadir-viewing High Spectral Resolution Lidar-2 (HSRL-2) data for vertically resolved "curtains" of aerosol extinction coefficient at 532 nm. The HSRL-2 instrument has been used in past airborne campaigns and readers are referred elsewhere for further information about its operational details (Burton et al., 2018).

To complement the analysis of the airborne data, the origin and type of the observed aerosol particles during the flight were identified using the combination of the NOAA Hybrid Single-Particle Lagrangian Integrated Trajectory (HYSPLIT) model (Rolph et al., 2017; Stein et al., 2015), MERRA-2 BC spatial data, and speciated AODs from the Navy Aerosol Analysis and Prediction System (NAAPS) (Lynch et al., 2016; https://www.nrlmry.navy.mil/aerosol/). HYSPLIT 96 hr back-trajectories were obtained for different points and times in the flight using GDAS meteorological data and the Model Vertical Velocity method. NAAPS is based on meteorological data from the Navy Global Environmental Model (NAVGEM; Hogan et al., 2014).

2.6. Cloud Properties

For an assessment of cloud characteristics in this study, we use properties from the MODerate resolution Imaging Spectroradiometer (MODIS), on Aqua, as part of the Clouds and the Earth's Radiant Energy System (CERES) Edition 4 (Loeb et al., 2016), with cloud algorithms described in Minnis et al. (2011, 2021) and Trepte et al. (2019). Here, we use the Level 3 Single Scanning Footprint (SSF) cloud product, which corresponds to pixel-level cloud properties averaged to a spatial resolution of 1° × 1°. We further use the CERES-MODIS subset for grids with averaged cloud retrievals featuring cloud heights below 700 hPa. Cloud properties used in this study for the 2005–2018 period include: cloud effective radius (r_e), cloud fraction, liquid water path (LWP), and cloud optical depth (τ). Cloud droplet number concentration (N_d) was additionally calculated based on the following equation (Painemal & Zuidema, 2011):

$$N_d = 1.4067 \times 10^{-6}\left[\ \mathrm{cm}^{-0.5}\right] \times \frac{\tau^{0.5}}{r_e^{2.5}} \quad (1)$$

The 1.4067×10^{-6} constant in the equation has the parameter k (related to the width of the droplet size distribution) embedded as 0.8, which instead is assumed to be 0.67 here for the East Coast sub-domains (NE, MA-N, MA-S, SE) as this value has been suggested to be better suited over land (Martin et al., 1994). We still use 0.8 for the Bermuda sub-domain as it is over the open ocean. Data are only used when liquid cloud fraction exceeded 30% to reflect a balance between reliability of retrieval data and maintaining a reasonable sample size. MODIS cloud products can be biased when an optically thick BB layer is located above the cloud, as the algorithm does account for the radiative properties of the overlying aerosol particles. These MODIS biases have been well documented over the southeast Atlantic during the BB season (e.g., Meyer et al., 2013). However, these artifacts were minimized in our study as we used r_e retrievals based on the 3.78-μm, channel, which has proven to be nearly insensitive to the effect of absorbing particles (Haywood et al., 2004), as well as less affected by spatial inhomogeneities and 3-D radiative transfer effects than the commonly used 2.13-μm channel (e.g., Painemal et al., 2013; Zhang & Platnick, 2011). Given the dependence of LWP and N_d on r_e, it follows that our MODIS data set is less sensitive to artifacts associated with BB particles above clouds.

3. Results

3.1. Temporal Variations

The occurrence of BB days was examined on seasonal (Figure 2) and interannual (Figure 3 and Figure S2 in Supporting Information S1) time scales. Each sub-domain has more frequent BB days in warmer months (May–September), followed by a decline in colder months (November–February). The June-July-August (JJA) season coincided with the highest frequency of BB days in sub-domains NE, MA-N, and MA-S, whereas Bermuda and SE regions exhibited the most BB days in the March-April-May (MAM) season (Figure 2). The December-January-February (DJF) season had the fewest BB days of any season

for all sub-domains likely driven by the lack of large-scale events in source regions such as western North America and Mexico.

Figure 3 depicts the average monthly frequency of occurrence for BB days over each sub-domain for two periods: 2005–2011 and 2012–2018. Sub-domain SE exhibited more BB days in 2012–2018 (227) relative to 2005–2011 (162). In contrast, the number of BB days was more comparable between the two time periods for the other sub-domains (2005–2011/2012–2018): NE = 178/171, MA-N = 231/230, MA-S = 258/232, Bermuda = 158/150. Figure S2 in Supporting Information S1 shows how the number of BB days varied by year from 2005 to 2018. Sub-domain SE shows the only pronounced trend over time with a progressive increase in BB days starting especially in 2009 (19 days) after which there is a near doubling of events in 2018 (36 days). The months between November and April were particularly influential in the enhanced frequency of BB days for sub-domain SE in more recent years (Figure 3); these months coincide with extensive agricultural burning in the southeast U.S. around Florida (Le Blond et al., 2017; Ma et al., 2014) and also prescribed burning (Olson & Platt, 1995; Platt et al., 2015). Using National Environmental Satellite Data, and Information System Hazard Mapping System (HMS) data, Brey et al. (2018) reported that the fire season in the southeastern U.S. is bimodal with the largest peak between January and April primarily due to debris burning, with a second peak in November also linked predominantly to human-induced burning. Kim et al. (2020) observed extensive fires over the southeast U.S. in November 2016, which stood out as being more extensive than anywhere else in the U.S. for that month. Jaffe et al. (2020) also reported extensive fire activity across the southeast U.S. in the winter and late fall. Although such fires in the southeast U.S. are smaller than wildfires over the western U.S., they significantly degrade air quality because of the large number of such fires (Brey et al., 2018). Furthermore, prescribed burning in the southeast U.S. is thought to lean more toward smoldering conditions as compared to other parts of the U.S., but there are conflicting views as to whether $PM_{2.5}$ emission factors are higher or lower compared to other parts of the U.S. (Jaffe et al., 2020; Liu et al., 2017; Prichard et al., 2020). Although not the focus of this work, future efforts would be worthwhile to disentangle the effects of changing emissions versus atmospheric transport and weather-related factors when examining interannual trends.

3.2. BB Spatial Extent

To isolate regions acting as sources and transport corridors leading to BB days for each receptor sub-domain, we use two types of spatial maps. We show spatial maps of BC anomaly, computed as the difference between the mean MERRA-2 BC value on BB days in a given season and the mean value of all days in that season (Figure 4). Hashed areas in Figure 4 indicate grids where the anomaly value is statistically significant with 95% confidence based on the Student's *t*-test for a given season. The second type of map is for associated seasonal composites of BC values for BB days (Figures S3–S6 in Supporting Information S1). MERRA-2 BC data are advantageous for these maps owing to broad spatial coverage as compared to surface monitoring networks such as AERONET.

Figure 2 already showed that MAM and JJA were the two seasons with the most BB days, with more in JJA toward the north (sub-domains NE/MA-N/MA-S) and more over

Bermuda and SE in MAM. The fractional occurrence of BB days occurring in JJA/MAM versus BB days across the entire year are 0.54/0.23, 0.48/0.25, and 0.46/0.29 for NE, MA-N, and MA-S, respectively, as compared to 0.30/0.43 and 0.38/0.43 for SE and Bermuda, respectively. Bermuda's position far from the East Coast with somewhat similar air patterns in MAM and JJA (Aldhaif et al., 2021; Corral et al., 2021) results in greater similarity in BB frequency in these two seasons as compared to other sub-domains. Figure 4a and Figure S3 in Supporting Information S1 show that during MAM, concentrated areas of most enhanced BC were over Mexico, especially the southern part and the Yucatan peninsula, and also over Central America. These areas are known to be active BB sources in MAM (Gupta et al., 2018; Kreidenweis et al., 2001; Roy et al., 2018; Wang et al., 2006; Yokelson et al., 2009). The hashed areas associated with the analysis for sub-domain SE suggest a transport corridor from Mexico and Central America toward the southeast U.S. and farther over the WNAO toward Bermuda. Other work has shown that agricultural burning in Meso and Central American countries yields extensive smoke occurrence in MAM over the Eastern U.S. assisted in part by the Bermuda high-pressure system southeast of Florida (Kaulfus et al., 2017). Florida itself is shown to have anomalously high BC values due likely to agricultural burning (Corral et al., 2020; Dennis et al., 2002; McCarty et al., 2007; Mendoza et al., 2005; Mitchell et al., 2014; Sevimoğlu & Rogge, 2019; Washenfelder et al., 2015). Relative to other parts of the U.S., the southeastern parts (especially Florida) exhibited the largest difference in mean $PM_{2.5}$ between smoke-influenced and smoke-free days due to some presumed combination of prescribed burns and wildfires (Kaulfus et al., 2017). In their analysis of fires in the year 2007, Rolph et al. (2009) found that the southeast U.S. accounted for the majority of fires across the country due partly to unusually dry conditions. Results for Bermuda show that BB transport predominantly comes from the outflow of the U.S. East Coast and Mexico.

In sharp contrast to MAM, the JJA results (Figure 4b and Figure S4 in Supporting Information S1) reveal a different spatial pattern with maxima in BC mainly located in the western parts of Canada and northwestern parts of U.S. Extensive past works have also identified these areas as BB sources due to wildfires (Boulanger et al., 2017; Dadashazar et al., 2019; Garofalo et al., 2019; Jaffe et al., 2008; Kaulfus et al., 2017; Mardi et al., 2018, 2019; Schlosser et al., 2017). The western U.S. appears to contribute less than Canada in these months, at least partly due to characteristic weather and transport patterns bringing air masses to the U.S. East Coast (e.g., DeBell et al., 2004; Dreessen et al., 2016; Li et al., 2005; Rogers et al., 2020). The analysis for sub-domain SE stands out with anomalously high BC values across the southeast U.S. and northwestern parts of North America, coincident with reduced levels over Mexico and Central America. It is not uncommon for smoke in the JJA season to move offshore the U.S. East Coast and then be pulled back inland owing to atmospheric circulations (DeBell et al., 2004).

The number of BB days during the September-October-November (SON) season expressed as a fraction of total BB days per year is as follows (Figure 2): 0.18 (NE), 0.22 (MA-N), 0.21 (MA-S), 0.13 (Bermuda), and 0.16 (SE). The highest numbers of BB days are linked to MA-N (101) and MA-S (103). In contrast, the lowest number (41 BB days) was for Bermuda, owing to its remote location farther away from BB sources. The spatial

distribution of BC (Figure 4c and Figure S5 in Supporting Information S1) is suggestive of influence from sources over the eastern U.S., northwestern U.S., and Canada.

The number of BB days is lowest for the DJF season, accounting for 4%–10% of total BB days on an annual basis for the five sub-domains (Figure 2). The peculiarly distinct and wide band of BC values by the U.S.-Canada border is due to the limited data points for this season biased by a major event stemming from western North America (Figure 4d and Figure S6 in Supporting Information S1). There were fewer areas of high BC as compared to other seasons, with regional sources over the eastern U.S. likely being influential. Based on analysis with the HMS fire and smoke product, widespread smoke was not observed in DJF over the U.S. except a few select areas including the Florida panhandle and Lake Okeechobee in southeastern Florida owing largely to prescribed burning (Kaulfus et al., 2017). Jaffe et al. (2020) also concluded based on satellite data that fires are mainly found in the southeast U.S. during DJF as compared to the rest of the U.S. as a result of prescribed burning. Similar to SON, Bermuda appears to be most impacted by areas of high BC north of North Carolina consistent with characteristic transport trajectories in those months (Aldhaif et al., 2021; Painemal et al., 2021). A noteworthy and consistent result across all seasons is that the influence of BB is evident offshore across the WNAO.

3.3. Surface Air Quality

The impact of BB on surface air quality over the U.S. East Coast is well documented (Bein et al., 2008, 2020; Colarco et al., 2004; DeBell et al., 2004; Dreessen et al., 2016; Hung et al., 2020; Jeong et al., 2004; Rogers et al., 2020; Sapkota et al., 2005; Taubman et al., 2004; Wotawa & Trainer, 2000; Wu et al., 2018). For example, plumes from Canadian wildfires can entrain into the surface layer of a wide swath of the East Coast including the southeastern parts (Wotawa & Trainer, 2000) and northern areas such as Washington, DC (Colarco et al., 2004), Maryland (Dreessen et al., 2016), New York (Hung et al., 2020; Rogers et al., 2020), Pennsylvania (Bein et al., 2008), Connecticut (Rogers et al., 2020), and Maine (DeBell et al., 2004). Northeastern U.S. surface air quality can additionally be impacted by air masses passing over active fires in the southeast U.S. (Rogers et al., 2020). The following analysis aims to examine what fraction of BB days with available IMPROVE data yielded anomalously high deseasonalized $PM_{2.5}$ levels (called BB + $PM_{2.5}$ days) for each surface station (shown in Figure 1; note again Bermuda does not have IMPROVE data and is excluded from this analysis). We additionally compare mass concentrations of important aerosol constituents ($PM_{2.5}$, PM_{10}, EC, OC, SO_4^{2-}, and K) between non-BB days with available IMPROVE data and BB + $PM_{2.5}$ days. We present results for both the full study period (Figure 5) and each season (Tables S7–S10 in Supporting Information S1).

For the full study period, the 14 IMPROVE stations exhibited between 22% and 42% agreement in terms of how many BB days with available IMPROVE data also had anomalously high $PM_{2.5}$ based on the method described in Section 2.3. Reasons for low agreement include the strict criteria we use for BB days in addition to how the criteria are based on parameters relevant to the entire atmospheric column rather than the surface layer alone; however, these percentages indicate that our criteria still identified BB air masses sufficiently large in vertical extent to impact surface air quality. The mean (±standard

deviation) of agreement percentages were as follows for the sub-domains: 38 ± 2% (NE), 31% ± 7% (MA-N), 30% ± 6% (MA-S), and 29% ± 2% (SE). There was especially good correspondence between IMPROVE stations in NE and SE regions for BB + $PM_{2.5}$ days based on the smaller standard deviations; the generally low standard deviations indicate that the BB air masses detected with our criteria were spatially large and usually impacted all stations within a given sub-domain. When examined on a seasonal basis, agreement based on all 14 stations was as follows: 29% ± 12% (DJF), 22% ± 5% (MAM), 37% ± 6% (JJA), and 35% ± 14% (SON). Therefore, there was no major variation based on season with consistent features also being the lowest standard deviations in regions NE and SE for the seasons with the most BB days (MAM and JJA). The BB air masses in DJF and SON presumably were not as large as those in MAM and JJA leading to more spatial heterogeneity in terms of high $PM_{2.5}$ levels at different IMPROVE stations within a given sub-domain. For comparison, an independent study for the entire U.S. relying on the NOAA HMS data product found at least 20.1% of daily NAAQS exceedances (24 hr average NAAQS standard = 35 μg m^{-3}) to coincide with identifiable smoke plumes aloft, with the majority of such days in JJA and SON, and the fewest in DJF (Kaulfus et al., 2017).

The comparison of mass concentrations between non-BB days and BB + $PM_{2.5}$ days reveals, with two exceptions (Everglades for OC and Presque Isle for K), statistically significant enhancements for all species and sites on BB + $PM_{2.5}$ days for the cumulative time period. Based on 24 h data from all stations, $PM_{2.5}$ exhibited mean levels of 14.99 and 5.43 μg m^{-3} on BB + $PM_{2.5}$ and non-BB days, respectively. Other studies over the U.S. East Coast have reported similar relative amounts of $PM_{2.5}$ enhancement, including for an August 2018 smoke event over New York resulting in $PM_{2.5}$ to increase threefold from 8.4 to 24.8 μg m^{-3} (Hung et al., 2020). $PM_{2.5}$ increased by nearly a factor of 3 (26–71 μg m^{-3}) for a Canadian forest fire episode impacting Philadelphia, Pennsylvania (Jeong et al., 2004), with OC and SO_4^{2-} being significantly enhanced. $PM_{2.5}$ increased from ~5 to 25–30 μg m^{-3} upon the arrival of smoke to New York City from wildfires over Alberta, Canada, with enhancements in OC, EC, and K^+ (Wu et al., 2018). Edwards et al. (2021) showed a twofold increase in $PM_{2.5}$ when comparing BB days (9.54 μg m^{-3}) to background days (4.26 μg m^{-3}) in coastal southeast Florida. In contrast with the previous studies, Sapkota et al. (2005) reported much higher $PM_{2.5}$ enhancements over Baltimore (8-fold increase relative to background) during the arrival of BB plumes from Quebec forest fires in July 2002, with the 24 h $PM_{2.5}$ concentration reaching as high as 86 μg m^{-3}.

Sulfate exhibited the highest mean enhancement on BB + $PM_{2.5}$ days when accounting for all sites (304 ± 55%), followed by $PM_{2.5}$ (281 ± 28%), OC (272 ± 49%), EC (230 ± 43%), PM_{10} (222 ± 29%), and K (200 ± 49%). The strong SO_4^{2-} enhancement on BB days is noteworthy as Bian et al. (2020) previously showed that smoke in the southeast U.S. has a higher SO_4^{2-} fraction than smoke over the western U.S. Furthermore, Bian et al. (2020) showed that southeastern U.S. smoke aerosol exhibited greater variability in optical properties than the western U.S. due to more varied sources (e.g., fresh and aged/transported smoke) as compared to fresher smoke over the western U.S.

The commonly used BB marker potassium (K) (e.g., Artaxo et al., 1994; Calloway et al., 1989; Pósfai et al., 2003; Reid et al., 2005) was two times as abundant on BB + $PM_{2.5}$

days (0.08 μg m^{-3}) as compared to non-BB days (0.04 μg m^{-3}) for the full study period when considering all sites together, supportive of the accurate detection of BB air masses with the study's BB identification criteria. Results on a seasonal basis mostly resemble those of the full time period in that there were statistically significant enhancements in species concentrations on BB + $PM_{2.5}$ days with some variability in terms of what species were most enhanced depending on season and sub-domain (Tables S7–S10 in Supporting Information S1). Varying relative levels of species such as OC, EC, SO_4^{2-}, and K on BB + $PM_{2.5}$ days for different sites and seasons are expected based on different influential fuel types, flame conditions, and aging/transport characteristics (Akagi et al., 2011; Lee et al., 2010; Pratt et al., 2011). Although this section showed that BB air masses transported from long distances can impact the surface layer, the next section looks more closely at the vertical profile of aerosol on BB days in contrast to non-BB days using remote sensing data.

3.4. Vertical BB Characteristics

Seasonal mean aerosol extinction profiles for BB and non-BB days are compared for the period between June 2006 and December 2018 (nighttime and daytime data in Figure 6 and Figure S7 in Supporting Information S1, respectively). Because of improved CALIOP signal to noise ratios at night and greater sensitivity to faint aerosol layers relative to daytime observations (Tackett et al., 2018), we focus the discussion below on nighttime observations (Figure 6), and refer interested readers to view qualitatively similar daytime results in Figure S7 in Supporting Information S1. The mean profiles generally reveal an aerosol extinction enhancement for BB days for both daytime and nighttime conditions up to approximately 5 km, with differences more pronounced with nighttime data. Unlike other seasons, DJF tended to exhibit more similar aerosol extinction values between BB and non-BB days, albeit with high variability indicated by the shading. Bermuda exhibited the lowest difference in extinction between BB and non-BB days as it is farthest away from BB sources.

For comparison with these results, the majority of smoke from a Canadian forest fire impacting the eastern U.S. was initially injected into a 2–6 km altitude band near Quebec and then subsided such that the plume was concentrated between 2 and 3 km over the Washington, DC area (Colarco et al., 2004). In a case study of BB plumes originating over Alaska and Yukon and being transported to Nova Scotia, aerosol layers reached up to 8 km (Duck et al., 2007). Taubman et al. (2004) reported BB plumes between 2 and 3 km over Virginia and Maryland based on airborne measurements of advected BB plumes from Quebec forest fires in July 2002. Others have shown smoke plumes from Canada advected to the U.S. East Coast reside in the bottom 5 km (DeBell et al., 2004; Dreessen et al., 2016; McKeen et al., 2002). Western North American wildfire plumes advected to New York resulted in BB aerosol around 2–5 km (Hung et al., 2020). BB plumes reaching New York in August 2018 originated near the surface (≤1.5 km) over the southeastern U.S. where there was likely crop burning (Rogers et al., 2020).

The MA-S sub-domain in JJA is especially of interest as it exhibited the highest aerosol extinction values up to 4 km on BB days based on nighttime data as compared to any other sub-domain or season. An example of a representative BB air mass in sub-domain MA-S

is shown in Figure 7, based on airborne King Air HSRL-2 data obtained in ACTIVATE's Research Flight 28 on 26 August 2020. This was a ~3.8 hr flight (13:54–17:41 UTC) with a southeast heading from Langley Air Force Base over the WNAO, followed by a reverse heading to re-trace the flight track back to the airfield. The HSRL-2 data are from the second half of the flight on the reverse track back to the airfield. While there are appreciable aerosol extinction coefficient values in the marine boundary layer, there are notably high values in the free troposphere (>2 km), reaching up to as high as 8 km by the coastline. These results can help explain why IMPROVE data agreement on BB days was ≤53% depending on the site and season, due to BB particles residing above the surface layer. The altitudes of BB plumes detected in this research flight are consistent with the previous reports of BB layer altitudes mentioned above.

Figure 7 shows supporting evidence that the source of the enhanced aerosol extinction aloft in the free troposphere is transported wildfire emissions from the western U.S. based on smoke optical depths from NAAPS, BC from MERRA-2, and HYSPLIT back-trajectories from different points during the flight. Subsequent, more detailed work will examine lidar data from the King Air and in situ data from the HU-25 Falcon to diagnose compositional characteristics in different vertical layers to better constrain the layering characteristics of smoke. However, a key conclusion from the combined data in Figure 7 and the CALIOP analysis is that smoke can extend over a broad range of altitudes over the U.S. East Coast and WNAO with important implications for clouds extending from the boundary layer to the upper troposphere. More specifically, Figure 7 shows areas of enhanced aerosol extinction from smoke overlapping with clouds extending to around ~2.5 km. This case flight demonstrates that smoke particles can both directly interact with clouds (i.e., co-located) and potentially even indirectly when residing above clouds via their ability to absorb radiation, increase lower tropospheric stability, and suppress vertical entrainment of dry air (e.g., Ackerman et al., 2000; Brioude et al., 2009; Hansen et al., 1997; Johnson et al., 2004; Kaufman et al., 2005). The next section examines cloud characteristics in different conditions as they relate to BB influence.

3.5. Cloud Characteristics

Interactions between aerosol particles and clouds constitute the largest uncertainty in estimates of total anthropogenic forcing (IPCC, 2013), motivating analysis of the relationships between smoke particles and clouds in the study region. Interactions between smoke and clouds are poorly understood and are thought to vary depending on the position of smoke relative to clouds (Brioude et al., 2009; Johnson et al., 2004). The goal of our cloud analysis is to determine whether changes in cloud properties for BB events are potentially indicative of aerosol-cloud interactions.

Table 1 compares values of CERES-MODIS cloud fraction, LWP, and two microphysical variables (N_d, r_e) between BB and non-BB days for low-level liquid clouds for each season and sub-domain. We additionally examine cloud characteristics of two portions of the BB days, including those with anomalously high surface $PM_{2.5}$ levels (called BB + $PM_{2.5}$ days) and all the remaining BB days (called BB−$PM_{2.5}$ days), as described in Section 2.3. The cloud statistics we report are based on entire sub-domain values, whereas IMPROVE and

AERONET data are at specific points and thus there could be varying degrees of smoke influence on clouds within a sub-domain. We speculate that BB + $PM_{2.5}$ days have a greater likelihood of BB particles interacting with low-level liquid clouds. Table S11 in Supporting Information S1 reports number of points used for the analysis in Table 1, which is important as some categories have ≤5 data points after applying the strict criteria for BB + $PM_{2.5}$ days (especially DJF), including how low-level cloud fraction had to exceed 30% based on Section 2.6. Given the modest number of available samples for BB + $PM_{2.5}$ and BB−$PM_{2.5}$ days (Table S11 in Supporting Information S1), we focus most of the discussion on comparing non-BB and BB days irrespective of $PM_{2.5}$ (Table 1), and interested readers can view results for BB + $PM_{2.5}$ and BB−$PM_{2.5}$ in Table S12 in Supporting Information S1. Moreover, we focus most of our attention on the All category (i.e., all seasons combined) to circumvent the limited seasonal sampling, especially in DJF.

Keeping in mind that our method applied a minimum threshold of 30%, mean cloud fractions were between 38% and 48% depending on the sub-domain and air mass category, constraining the range of cloud cover variability. Both cloud fraction and LWP are generally higher for non-BB days, with statistically significant results observed over the NE and Bermuda regions for both cloud variables. The NE region also had a significant reduction in LWP for BB + $PM_{2.5}$ days (73 g m^{-2}) as compared to non-BB days (120 g m^{-2}), with BB−$PM_{2.5}$ days having an intermediate mean value (97 g m^{-2}) (Table S12 in Supporting Information S1). While meteorological factors have not been held fixed, this result of lower LWP and cloud fraction on BB days is at least consistent with the expectation that smoke particles containing soot readily absorb sunlight, with the radiative heating ultimately leading to cloud thinning and dissipation (e.g., Ackerman et al., 2000). N_d is next analyzed to assess if an enhancement was observed on BB days as this parameter represents the most direct microphysical response of clouds to aerosol perturbations. N_d values were significantly higher on BB days versus non-BB days, except for MA-S where there was an enhancement but not at a 95% confidence level. Moreover, the N_d enhancement on BB days is consistently observed for all seasons but with smaller differences in JJA as the region features an N_d annual minimum in summer (Dadashazar, Painemal, et al., 2021; Painemal et al., 2021). While the analysis suggests a tie between BB days and cloud microphysics, co-variability between BC and other species cannot be fully disentangled. As already shown, BB days feature high surface concentrations of species such as OC and SO_4^{2-} (Figure 5), suggesting the presence of CCN originating from different precursors.

Higher values of N_d at fixed LWP generally are expected to result in reductions in r_e (Twomey, 1977). Owing to the limited sample size of BB days, r_e values are first examined without binning by LWP. Values of r_e agree with N_d in that BB days are associated with a significant decrease (increase) in r_e (N_d), with the exception of the SE region where the r_e reduction was not significant at the 95% confidence level. We further examined differences in N_d and r_e in three bins of LWP (80–110, 110–170, and 170–270 g m^{-2}) (Table S13 in Supporting Information S1), with results from Table 1 for N_d and r_e generally preserved, including lower r_e and higher N_d on BB days, regardless of LWP value. An aspect unexplored in this study is the role of precipitation, which could be responsible for aerosol scavenging under the presence of large droplet sizes, and possibly explaining part of the relationships in Table 1. Based on the precipitation analysis in Kawamoto and Suzuki

(2013), moderate precipitation typically occurs for LWP > 200 g m^{-2}, and drizzle for LWP > 100 g m^{-2} and N_d < 50 cm^{-3}. It follows that for the clouds analyzed here (Table 1), drizzle and non-precipitating clouds were likely dominant, thus making it less plausible that aerosol scavenging by precipitation is the dominant factor explaining differences in cloud properties between BB and non-BB days.

This analysis leaves open questions to address with future data sets and analyses grounded on more statistics and resolution to examine processes near and around clouds such as with airborne measurements. The cloud property analysis was limited in that the data set was not sufficiently large to allow for detailed analysis of the impact of various meteorological influences such as (but not limited to): subsidence and boundary-layer stability (Klein & Hartmann, 1993; Kubar et al., 2012; Myers & Norris, 2013; Naud et al., 2016), sea surface temperature and surface heat fluxes (Painemal et al., 2021), and atmospheric circulation patterns (Li et al., 2005; Painemal et al., 2021). Motivated by the contrast between cloud parameters on non-BB and BB days between coastal and offshore areas, it is of interest to examine whether aerosol-cloud interaction signatures are weakened farther offshore over the WNAO (e.g., Bermuda) due to the presence of dissimilar meteorological regimes and aerosol scavenging (Dadashazar, Alipanah, et al., 2021) as the plumes move more than 1,000 km away from the continent.

4. Conclusions

This study used a combination of data sets to examine characteristics of BB air masses over the U.S. East Coast and the WNAO between 2005 and 2018. Using anomalously high deseasonalized values (upper decile) of AERONET AOD and MERRA-2 BC column density on a given day as criteria to detect BB days over five individual sub-domains, the following selected results emerged:

1. JJA and MAM had the most BB days, regardless of region, with more such cases to the north (sub-domains NE, MA-N, MA-S) in JJA and more over SE and Bermuda in MAM. In contrast, DJF exhibited the fewest BB days due to reduced influence from large-scale events that our classification methodology is biased toward.
2. For the seasons with most BB days, the most impactful source regions were either Mexico, Central America, and the southeast U.S. (MAM), or western North America (JJA). Noteworthy is that Bermuda had BB days in each season indicating that there is year-round influence from sources over North and Central America.
3. Although our classification criteria were biased toward large-scale events with high potential to reside aloft in the free troposphere, it was shown that for 14 IMPROVE sites across the U.S. East Coast there was 22%–42% agreement in terms of how many BB days with available IMPROVE data also had anomalously high $PM_{2.5}$ in the surface layer. A comparison of mass concentrations for selected IMPROVE parameters ($PM_{2.5}$, PM_{10}, SO_4^{2-}, OC, EC, and K) on those surface-impacted days relative to non-BB days revealed

enhancements between 200% and 304% based on all sites and the full study period.

4. The combination of both CALIOP and airborne HSRL-2 data confirms that smoke can impact the troposphere from the boundary layer to the upper troposphere (~8 km). A case flight from ACTIVATE on 26 August 2020 shows that smoke in the free troposphere originated over the western U.S. and interacted with clouds both directly by mixing and potentially indirectly with layers residing above clouds

5. Aerosol-cloud interactions were probed by binning data into separate categories based on non-BB days and BB days in each sub-domain on the East Coast and over Bermuda. Our results indicate there is a possible signature of aerosol-cloud interactions over the U.S. East Coast and the WNAO owing to appreciable N_d enhancement (and r_e reduction) on BB days and that smoke can likely impact clouds either if above them or entrained into them. Unfortunately, separating the contribution of boundary layer and free tropospheric aerosol particles cannot be achieved with our data set. In addition, reductions in LWP and cloud fraction on BB days are possibly linked to the heating effect of absorbing aerosol particles, contributing to cloud thinning and dissipation. However, testing this hypothesis will require a careful analysis of the meteorological factors associated with BB events, aided with numerical models, and more accurate observations from airborne in-situ probes

Supplementary Material

Refer to Web version on PubMed Central for supplementary material.

Acknowledgments

This study was funded by NASA Grant 80NSSC19K0442 in support of the ACTIVATE Earth Venture Suborbital-3 (EVS-3) investigation, which is funded by NASA's Earth Science Division and managed through the Earth System Science Pathfinder Program Office. Partial funding is also acknowledged from ONR grant N00014-21-1-2115. The authors acknowledge the NOAA Air Resources Laboratory (ARL) for the provision of the HYSPLIT transport and dispersion model and READY website (http://ready.arl.noaa.gov) used in this work.

Data Availability Statement

All data used in this work can be found at the following sites: NASA Atmospheric Infrared Sounder (AIRS): http://dx.doi.org/10.5067/AQUA/AIRS/DATA202. NASA Ozone Monitoring Instrument (OMI): http://dx.doi.org/10.5067/MEASURES/AER/DATA203. NASA Modern-Era Retrospective analysis for Research and Applications, Version 2 (MERRA-2): http://dx.doi.org/10.5067/KLICLTZ8EM9D. NASA AErosol RObotic NETwork (AERONET): https://aeronet.gsfc.nasa.gov/new_web/download_all_v3_aod.html. Interagency Monitoring of Protected Visual Environments (IMPROVE): http://views.cira.colostate.edu/fed/SiteBrowser/Default.aspx. ACTIVATE aircraft data: https://www-air.larc.nasa.gov/missions/activate/index.html. NASA Cloud-Aerosol Lidar with Orthogonal Polarization (CALIOP): https://subset.larc.nasa.gov/calipso. NASA CERES-MODIS: https://ceres.larc.nasa.gov/data/.

References

Abatzoglou JT, & Williams AP (2016). Impact of anthropogenic climate change on wildfire across western US forests. Proceedings of the National Academy of Sciences of The United States of America, 113(42), 11770–11775. 10.1073/pnas.1607171113 [PubMed: 27791053]

Ackerman AS, Toon OB, Stevens DE, Heymsfield AJ, Ramanathan V, & Welton EJ (2000). Reduction of tropical cloudiness by soot. Science, 288(5468), 1042–1047. 10.1126/science.288.5468.1042 [PubMed: 10807573]

Akagi SK, Yokelson RJ, Wiedinmyer C, Alvarado MJ, Reid JS, Karl T, et al. (2011). Emission factors for open and domestic biomass burning for use in atmospheric models. Atmospheric Chemistry and Physics, 11(9), 4039–4072. 10.5194/acp-11-4039-2011

Aldhaif AM, Lopez DH, Dadashazar H, Painemal D, Peters AJ, & Sorooshian A (2021). An aerosol climatology and implications for clouds at a remote marine site: Case study over Bermuda. Journal of Geophysical Research: Atmospheres, 126(9), e2020JD034038. 10.1029/2020JD034038

Andreae MO (2019). Emission of trace gases and aerosols from biomass burning—An updated assessment. Atmospheric Chemistry and Physics, 19(13), 8523–8546. 10.5194/acp-19-8523-2019

Artaxo P, Gerab F, Yamasoe MA, & Martins JV (1994). Fine mode aerosol composition at three long-term atmospheric monitoring sites in the Amazon Basin. Journal of Geophysical Research, 99(D11), 22857–22868. 10.1029/94JD01023

Barbero R, Abatzoglou JT, Larkin NK, Kolden CA, & Stocks B (2015). Climate change presents increased potential for very large fires in the contiguous United States. International Journal of Wildland Fire, 24(7), 892–899. 10.1071/WF15083

Bein KJ, Zhao Y, Johnston MV, & Wexler AS (2008). Interactions between Boreal Wildfire and Urban Emissions. Journal of Geophysical Research: Atmospheres, 113(D7). 10.1029/2007jd008910

Berg LK, Fast JD, Barnard JC, Burton SP, Cairns B, Chand D, et al. (2016). The two-column aerosol project: Phase I overview and impact of elevated aerosol layers on aerosol optical depth. Journal of Geophysical Research-Atmospheres, 121(1), 336–361. 10.1002/2015JD023848

Bian Q, Ford B, Pierce JR, & Kreidenweis SM (2020). A decadal climatology of chemical, physical, and optical properties of ambient smoke in the Western and Southeastern United States. Journal of Geophysical Research-Atmospheres, 125(1). 10.1029/2019JD031372

Boulanger Y, Girardin M, Bernier PY, Gauthier S, Beaudoin A, & Guindon L (2017). Changes in mean forest age in Canada's forests could limit future increases in area burned but compromise potential harvestable conifer volumes. Canadian Journal of Forest Research, 47(6), 755–764. 10.1139/cjfr-2016-0445

Brey SJ, Barnes EA, Pierce JR, Wiedinmyer C, & Fischer EV (2018). Environmental conditions, ignition type, and air quality impacts of wildfires in the Southeastern and Western United States. Earth's Future, 6(10), 1442–1456. 10.1029/2018EF000972 [PubMed: 31008140]

Brioude J, Cooper OR, Feingold G, Trainer M, Freitas SR, Kowal D, et al. (2009). Effect of biomass burning on marine stratocumulus clouds off the California Coast. Atmospheric Chemistry and Physics, 9(22), 8841–8856. 10.5194/acp-9-8841-2009

Burton SP, Hostetler CA, Cook AL, Hair JW, Seaman ST, Scola S, et al. (2018). Calibration of a high spectral resolution Lidar using a Michelson Interferometer, with data examples from Oracles. Applied Optics, 57(21), 6061–6075. 10.1364/Ao.57.006061 [PubMed: 30118035]

Calloway CP, Li S, Buchanan JW, & Stevens RK (1989). A refinement of the potassium tracer method for residential wood smoke. Atmospheric Environment, 23(1), 67–69. 10.1016/0004-6981(89)90098-X

Chen LQ, & Duce RA (1983). The sources of sulfate, vanadium and mineral matter in aerosol-particles over Bermuda. Atmospheric Environment, 17(10), 2055–2064. 10.1016/0004-6981(83)90362-1

Chow JC, Lowenthal DH, Chen L-WA, Wang X, & Watson JG (2015). Mass reconstruction methods for $PM_{2.5}$: A review. Air Quality Atmosphere and Health, 8(3), 243–263. 10.1007/s11869-015-0338-3

Chow JC, Watson JG, Chen L-WA, Chang MCO, Robinson NF, Trimble D, & Kohl S (2007). The IMPROVE—A temperature protocol for thermal/optical carbon analysis: Maintaining consistency

with a long-term database. Journal of the Air & Waste Management Association, 57(9), 1014–1023. 10.3155/1047-3289.57.9.1014 [PubMed: 17912920]

Clarke A, McNaughton C, Kapustin V, Shinozuka Y, Howell S, Dibb J, et al. (2007). Biomass burning and pollution aerosol over North America: Organic components and their influence on spectral optical properties and humidification response. Journal of Geophysical Research-Atmospheres, 112(D12). 10.1029/2006JD007777

Colarco PR, Schoeberl MR, Doddridge BG, Marufu LT, Torres O, & Welton EJ (2004). Transport of smoke from Canadian forest fires to the surface near Washington, D. C.: Injection height, entrainment, and optical properties. Journal of Geophysical Research-Atmospheres, 109(D6). 10.1029/2003JD004248

Cook PA, Savage NH, Turquety S, Carver GD, O'Connor FM, Heckel A, et al. (2007). Forest fire plumes over the North Atlantic: P-TOMCAT model simulations with aircraft and satellite measurements from the ITOP/ICARTT campaign. Journal of Geophysical Research, 112(D10). 10.1029/2006JD007563

Corral AF, Braun RA, Cairns B, Gorooh VA, Liu H, Ma L, et al. (2021). An overview of atmospheric features over the Western North Atlantic Ocean and North American East Coast—Part 1: Analysis of aerosols, gases, and wet deposition chemistry. Journal of Geophysical Research: Atmospheres, 126(4). 10.1029/2020JD032592

Corral AF, Dadashazar H, Stahl C, Edwards E-L, Zuidema P, & Sorooshian A (2020). Source apportionment of aerosol at a coastal site and relationships with precipitation chemistry: A case study over the Southeast United States. Atmosphere, 11(11), 1212. 10.3390/atmos11111212 [PubMed: 34211764]

Crutzen PJ, & Andreae MO (1990). Biomass burning in the tropics—Impact on atmospheric chemistry and biogeochemical cycles. Science, 250(4988), 1669–1678. 10.1126/science.250.4988.1669 [PubMed: 17734705]

Dadashazar H, Alipanah M, Hilario MRA, Crosbie E, Kirschler S, Liu H, et al. (2021). Aerosol responses to precipitation along North American air trajectories arriving at Bermuda. Atmospheric Chemistry and Physics. 10.5194/acp-2021-471

Dadashazar H, Ma L, & Sorooshian A (2019). Sources of pollution and interrelationships between aerosol and precipitation chemistry at a central California site. The Science of the Total Environment, 651(2), 1776–1787. 10.1016/j.scitotenv.2018.10.086 [PubMed: 30316095]

Dadashazar H, Painemal D, Alipanah M, Brunke M, Chellappan S, Corral AF, & Sorooshian A (2021). Cloud drop number concentrations over the Western North Atlantic Ocean: Seasonal cycle, aerosol interrelationships, and other influential factors. Atmospheric Chemistry and Physics, 21. 10.5194/acp-21-1-2021

de Gouw JA, Warneke C, Stohl A, Wollny AG, Brock CA, Cooper OR, et al. (2006). Volatile organic compounds composition of merged and aged forest fire plumes from Alaska and western Canada. Journal of Geophysical Research Atmospheres, 111(10). 10.1029/2005JD006175

DeBell LJ, Talbot RW, Dibb JE, Munger JW, Fischer EV, & Frolking SE (2004). A major regional air pollution event in the Northeastern United States caused by extensive forest fires in Quebec, Canada. Journal of Geophysical Research-Atmospheres, 109(D19). 10.1029/2004jd004840

Dennis A, Fraser M, Anderson S, & Allen D (2002). Air pollutant emissions associated with forest, grassland, and agricultural burning in Texas. Atmospheric Environment, 36(23), 3779–3792. 10.1016/S1352-2310(02)00219-4

Dickerson RR, Doddridge BG, Kelley P, & Rhoads KP (1995). Large-scale pollution of the atmosphere over the remote Atlantic Ocean—Evidence from Bermuda. Journal of Geophysical Research, 100(D5), 8945–8952. 10.1029/95JD00073

Dreessen J, Sullivan J, & Delgado R (2016). Observations and impacts of transported Canadian wildfire smoke on ozone and aerosol air quality in the Maryland region on June 9–12, 2015. Journal of the Air & Waste Management Association, 66(9), 842–862. 10.1080/10962247.2016.1161674 [PubMed: 26963934]

Duck TJ, Firanski BJ, Millet DB, Goldstein AH, Allan J, Holzinger R, et al. (2007). Transport of forest fire emissions from Alaska and the Yukon Territory to Nova Scotia during summer 2004. Journal of Geophysical Research: Atmospheres, 112(D10). 10.1029/2006JD007716

Edwards E-L, Corral AF, Dadashazar H, Barkley AE, Gaston CJ, Zuidema P, & Sorooshian A (2021). Impact of various air mass types on cloud condensation nuclei concentrations along coastal Southeast Florida. Atmospheric Environment, 254, 118371. 10.1016/j.atmosenv.2021.118371 [PubMed: 34211332]

Fehsenfeld FC, Ancellet G, Bates TS, Goldstein AH, Hardesty RM, Honrath R, et al. (2006). International Consortium for Atmospheric Research on Transport and Transformation (ICARTT): North America to Europe – Overview of the 2004 summer field study. Journal of Geophysical Research-Atmospheres, 111(D23). 10.1029/2006JD007829

Garofalo LA, Pothier MA, Levin EJT, Campos T, Kreidenweis SM, & Farmer DK (2019). Emission and evolution of submicron organic aerosol in smoke from wildfires in the Western United States. ACS Earth and Space Chemistry, 3(7), 1237–1247. 10.1021/acsearthspacechem.9b00125

Gelaro R, McCarty W, Suarez MJ, Todling R, Molod A, Takacs L, et al. (2017). The modern-era retrospective analysis for research and applications, version 2 (MERRA-2). Journal of Climate, 30(14), 5419–5454. 10.1175/JCLI-D-16-0758.1 [PubMed: 32020988]

Gupta T, Agarwal AK, Agarwal RA, & Labhsetwar NK (2018). Environmental contaminants measurement, modelling and control preface. Springer-Verlag Singapore PTE LTD.

Hand JL, Schichtel BA, Malm WC, & Pitchford ML (2012). Particulate sulfate ion concentration and SO_2 emission trends in the United States from the early 1990s through 2010. Atmospheric Chemistry and Physics, 12(21), 10353–10365. 10.5194/acp-12-10353-2012

Hansen J, Sato M, & Ruedy R (1997). Radiative forcing and climate response. Journal of Geophysical Research-Atmospheres, 102(D6), 6831–6864. 10.1029/96jd03436

Haywood JM, Osborne SR, & Abel SJ (2004). The effect of overlying absorbing aerosol layers on remote sensing retrievals of cloud effective radius and cloud optical depth. Quarterly Journal of the Royal Meteorological Society, 130(598), 779–800. 10.1256/qj.03.100

Heald CL, Jacob DJ, Turquety S, Hudman RC, Weber RJ, Sullivan AP, et al. (2006). Concentrations and sources of organic carbon aerosols in the free troposphere over North America. Journal of Geophysical Research Atmospheres, 111(23), 1–12. 10.1029/2005JD007705 [PubMed: 20411040]

Hobbs PV, Reid JS, Kotchenruther RA, Ferek RJ, & Weiss R (1997). Direct radiative forcing by smoke from biomass burning. Science, 275(5307), 1776–1778. 10.1126/science.275.5307.1777 [PubMed: 9065398]

Hogan TF, Liu M, Ridout JA, Peng MS, Whitcomb TR, Ruston BC, et al. (2014). The Navy global environmental model. Oceanography, 27(3), 116–125. 10.5670/oceanog.2014.73

Holben BN, Eck TF, Slutsker I, Tanre D, Buis JP, Setzer A, et al. (1998). AERONET—A federated instrument network and data archive for aerosol characterization. Remote Sensing of Environment, 66(1), 1–16. 10.1016/S0034-4257(98)00031-5

Honrath RE, Owen RC, Val Martín M, Reid JS, Lapina K, Fialho P, et al. (2004). Regional and hemispheric impacts of anthropogenic and biomass burning emissions on summertime CO and O_3 in the North Atlantic lower free troposphere. Journal of Geophysical Research: Atmospheres, 109(24), 1–17. 10.1029/2004JD005147

Huang SL, Rahn KA, Arimoto R, Graustein WC, & Turekian KK (1999). Semiannual cycles of pollution at Bermuda. Journal of Geophysical Research-Atmospheres, 104(D23), 30309–30317. 10.1029/1999JD900801

Hung W, Shrestha B, Lu CS, Lin H, Grogan D, Hong J, et al. (2020). The impacts of transported wildfire smoke aerosols on surface air quality in New York State: A case study in summer 2018. Atmospheric Environment, 227, 117415. 10.1016/j.atmosenv.2020.117415

IPCC. (2013). Climate change 2013: The physical science basis. Cambridge University Press.

Jaffe DA, Hafner W, Chand D, Westerling A, & Spracklen D (2008). Interannual variations in $PM_{2.5}$ due to wildfires in the Western United States. Environmental Science & Technology, 42(8), 2812–2818. 10.1021/es702755v [PubMed: 18497128]

Jaffe DA, O'Neill SM, Larkin NK, Holder AL, Peterson DL, Halofsky JE, & Rappold AG (2020). Wildfire and prescribed burning impacts on air quality in the United States. Journal of the Air & Waste Management Association, 70(6), 583–615. 10.1080/10962247.2020.1749731 [PubMed: 32240055]

Jeong C-H, Lee D-W, Kim E, & Hopke PK (2004). Measurement of real-time $PM_{2.5}$ mass, sulfate, and carbonaceous aerosols at the multiple monitoring sites. Atmospheric Environment, 38(31), 5247–5256. 10.1016/j.atmosenv.2003.12.046

Johnson BT, Shine KP, & Forster PM (2004). The semi-direct aerosol effect: Impact of absorbing aerosols on marine Stratocumulus. Quarterly Journal of the Royal Meteorological Society, 130(599), 1407–1422. 10.1256/qj.03.61

Jongeward AR, Li Z, He H, & Xiong X (2016). Natural and anthropogenic aerosol trends from satellite and surface observations and model simulations over the North Atlantic Ocean from 2002 to 2012. Journal of the Atmospheric Sciences, 73(11), 4469–4485. 10.1175/jas-d-15-0308.1

Junghenn Noyes K, Kahn R, Sedlacek A, Kleinman L, Limbacher J, & Li Z (2020). Wildfire smoke particle properties and evolution, from space-based multi-angle imaging. Remote Sensing, 12(5), 769. 10.3390/rs12050769

Kaufman YJ, Koren I, Remer LA, Rosenfeld D, & Rudich Y (2005). The effect of smoke, dust, and pollution aerosol on shallow cloud development over the Atlantic Ocean. Proceedings of the National Academy of Sciences of the United States of America, 102(32), 11207–11212. 10.1073/pnas.0505191102 [PubMed: 16076949]

Kaulfus AS, Nair U, Jaffe D, Christopher SA, & Goodrick S (2017). Biomass burning smoke climatology of the United States: Implications for particulate matter air quality. Environmental Science & Technology, 51(20), 11731–11741. 10.1021/acs.est.7b03292 [PubMed: 28960063]

Kawamoto K, & Suzuki K (2013). Comparison of water cloud microphysics over mid-latitude land and ocean using CloudSat and MODIS observations. Journal of Quantitative Spectroscopy and Radiative Transfer, 122, 13–24. 10.1016/j.jqsrt.2012.12.013

Kim HC, Chai T, Stein A, & Kondragunta S (2020). Inverse modeling of fire emissions constrained by smoke plume transport using HYSPLIT dispersion model and geostationary satellite observations. Atmospheric Chemistry and Physics, 20(17), 10259–10277. 10.5194/acp-20-10259-2020

Kim M-H, Omar AH, Tackett JL, Vaughan MA, Winker DM, Trepte CR, et al. (2018). The CALIPSO version 4 automated aerosol classification and lidar ratio selection algorithm. Atmospheric Measurement Techniques, 11(11), 6107–6135. 10.5194/amt-11-6107-2018 [PubMed: 31921372]

Klein SA, & Hartmann DL (1993). The seasonal cycle of low stratiform clouds. Journal of Climate, 6(8), 1587–1606. 10.1175/1520-0442(1993)006<1587:tscols>2.0.co;2

Kreidenweis SM, Remer LA, Bruintjes R, & Dubovik O (2001). Smoke aerosol from biomass burning in Mexico: Hygroscopic smoke optical model. Journal of Geophysical Research, 106(D5), 4831–4844. 10.1029/2000JD900488

Kubar TL, Waliser DE, Li J-L, & Jiang X (2012). On the annual cycle, variability, and correlations of oceanic low-topped clouds with large-scale circulation using Aqua Modis and Era-Interim. Journal of Climate, 25(18), 6152–6174. 10.1175/jcli-d-11-00478.1

Le Blond JS, Woskie S, Horwell CJ, & Williamson B (2017). Particulate matter produced during commercial sugarcane harvesting and processing: A respiratory health hazard? Atmospheric Environment, 149, 34–46. 10.1016/j.atmosenv.2016.11.012

Lee T, Sullivan AP, Mack L, Jimenez JL, Kreidenweis SM, Onasch TB, et al. (2010). Chemical smoke marker emissions during flaming and smoldering phases of laboratory open burning of wildland fuels. Aerosol Science and Technology, 44(9), i–v. 10.1080/02786826.2010.499884

Li Q, Jacob DJ, Park R, Wang Y, Heald CL, Hudman R, et al. (2005). North American pollution outflow and the trapping of convectively lifted pollution by upper-level anticyclone. Journal of Geophysical Research: Atmospheres, 110(D10). 10.1029/2004JD005039

Liu X, Huey LG, Yokelson RJ, Selimovic V, Simpson IJ, Müller M, et al. (2017). Airborne measurements of Western U.S. wildfire emissions: Comparison with prescribed burning and air quality implications. Journal of Geophysical Research: Atmospheres, 122(11), 6108–6129. 10.1002/2016JD026315

Loeb NG, Manalo-Smith N, Su W, Shankar M, & Thomas S (2016). Ceres top-of-atmosphere earth radiation budget climate data record: Accounting for in-orbit changes in instrument calibration. Remote Sensing, 8(3), 182. 10.3390/rs8030182

Lynch P, Reid JS, Westphal DL, Zhang JL, Hogan TF, Hyer EJ, et al. (2016). An 11-year global gridded aerosol optical thickness reanalysis (V1.0) for atmospheric and climate sciences. Geoscientific Model Development, 9(4), 1489–1522. 10.5194/gmd-9-1489-2016

Ma S, Karkee M, Scharf PA, & Zhang Q (2014). Sugarcane harvester technology: A critical overview. Applied Engineering in Agriculture, 30(5), 727–739.

Malm WC, Schichtel BA, Pitchford ML, Ashbaugh LL, & Eldred RA (2004). Spatial and monthly trends in speciated fine particle concentration in the United States. Journal of Geophysical Research-Atmospheres, 109(D3). 10.1029/2003JD003739

Malm WC, Sisler JF, Huffman D, Eldred RA, & Cahill TA (1994). Spatial and seasonal trends in particle concentration and optical extinction in the United States. Journal of Geophysical Research-Atmospheres, 99(D1), 1347–1370. 10.1029/93JD02916

Mao YH, Li QB, Zhang L, Chen Y, Randerson JT, Chen D, & Liou KN (2011). Biomass burning contribution to black carbon in the Western United States Mountain Ranges. Atmospheric Chemistry and Physics, 11(21), 11253–11266. 10.5194/acp-11-11253-2011

Mardi AH, Dadashazar H, MacDonald AB, Braun RA, Crosbie E, Xian P, et al. (2018). Biomass burning plumes in the vicinity of the California Coast: Airborne characterization of physicochemical properties, heating rates, and spatiotemporal features. Journal of Geophysical Research: Atmospheres, 123(23), 13560–13582. 10.1029/2018JD029134

Mardi AH, Dadashazar H, MacDonald AB, Crosbie E, Coggon MM, Aghdam MA, et al. (2019). Effects of biomass burning on stratocumulus droplet characteristics, drizzle rate, and composition. Journal of Geophysical Research: Atmospheres, 124(22), 12301–12318. 10.1029/2019JD031159

Martin GM, Johnson DW, & Spice A (1994). The measurement and parameterization of effective radius of droplets in warm stratocumulus clouds. Journal of the Atmospheric Sciences, 51(13), 1823–1842. 10.1175/1520-0469(1994)051<1823:TMAPOE>2.0.CO;2

Martin MV, Honrath RE, Owen RC, Pfister G, Fialho P, & Barata F (2006). Significant enhancements of nitrogen oxides, black carbon, and ozone in the North Atlantic lower free troposphere resulting from North American Boreal Wildfires. Journal of Geophysical Research: Atmospheres, 111(D23). 10.1029/2006jd007530

McCarty JL, Justice CO, & Korontzi S (2007). Agricultural burning in the Southeastern United States detected by MODIS. Remote Sensing of Environment, 108(2), 151–162. 10.1016/j.rse.2006.03.020

McKeen SA, Wotawa G, Parrish DD, Holloway JS, Buhr MP, Hübler G, et al. (2002). Ozone production from Canadian Wildfires during June and July of 1995. Journal of Geophysical Research: Atmospheres, 107(D14), ACH 7–1–ACH 7–25. 10.1029/2001JD000697

Mead C, Herckes P, Majestic BJ, & Anbar AD (2013). Source apportionment of aerosol iron in the marine environment using iron isotope analysis. Geophysical Research Letters, 40(21), 5722–5727. 10.1002/2013GL057713

Mendoza A, Garcia MR, Vela P, Lozano DF, & Allen D (2005). Trace gases and particulate matter emissions from wildfires and agricultural burning in Northeastern Mexico during the 2000 fire season. Journal of the Air & Waste Management Association, 55(12), 1797–1808. 10.1080/10473289.2005.10464778 [PubMed: 16408684]

Meyer K, Platnick S, Oreopoulos L, & Lee D (2013). Estimating the direct radiative effect of absorbing aerosols overlying marine boundary layer clouds in the Southeast Atlantic using MODIS and CALIOP. Journal of Geophysical Research: Atmospheres, 118(10), 4801–4815. 10.1002/jgrd.50449

Milne PJ, Prados AI, Dickerson RR, Doddridge BG, Riemer DD, Zika RG, et al. (2000). Nonmethane hydrocarbon mixing ratios in continental outflow air from eastern North America: Export of ozone precursors to Bermuda. Journal of Geophysical Research: Atmospheres, 105(D8), 9981–9990. 10.1029/1999JD901117

Minnis P, Sun-Mack S, Chen Y, Chang FL, Yost CR, Smith WL, et al. (2021). Ceres Modis cloud product retrievals for edition 4—Part I: Algorithm changes. IEEE Transactions on Geoscience and Remote Sensing, 59(4), 2744–2780. 10.1109/TGRS.2020.3008866

Minnis P, Sun-Mack S, Young DF, Heck PW, Garber DP, Chen Y, et al. (2011). Ceres edition-2 cloud property retrievals using TRMM VIRS and Terra and Aqua MODIS data—Part I:

Algorithms. IEEE Transactions on Geoscience and Remote Sensing, 49(11), 4374–4400. 10.1109/TGRS.2011.2144601

Mitchell RJ, Liu Y, O'Brien JJ, Elliott KJ, Starr G, Miniat CF, & Hiers JK (2014). Future climate and fire interactions in the southeastern region of the United States. Forest Ecology and Management, 327, 316–326. 10.1016/j.foreco.2013.12.003

Müller D, Hostetler CA, Ferrare RA, Burton SP, Chemyakin E, Kolgotin A, et al. (2014). Airborne multiwavelength High Spectral Resolution Lidar (HSRL-2) observations during TCAP 2012: Vertical profiles of optical and microphysical properties of a smoke/urban haze plume over the northeastern coast of the US. Atmospheric Measurement Techniques, 7(10), 3487–3496. 10.5194/amt-7-3487-2014

Myers TA, & Norris JR (2013). Observational evidence that enhanced subsidence reduces subtropical marine boundary layer cloudiness. Journal of Climate, 26(19), 7507–7524. 10.1175/jcli-d-12-00736.1

Naud CM, Booth JF, & Del Genio AD (2016). The relationship between boundary layer stability and cloud cover in the post-coldfrontal region. Journal of Climate, 29(22), 8129–8149. 10.1175/jcli-d-15-0700.1 [PubMed: 29983481]

Olson MS, & Platt WJ (1995). Effects of habitat and growing season fires on resprouting of shrubs in Longleaf Pine Savannas. Vegetatio, 119(2), 101–118. 10.1007/BF00045593

Painemal D, Corral AF, Sorooshian A, Brunke MA, Chellappan S, Afzali Gorooh V, et al. (2021). An overview of atmospheric features over the Western North Atlantic Ocean and North American East Coast – Part 2: Circulation, boundary layer, and clouds. Journal of Geophysical Research: Atmospheres, 126. 10.1029/2020JD033423

Painemal D, Minnis P, & Sun-Mack S (2013). The impact of horizontal heterogeneities, cloud fraction, and liquid water path on warm cloud effective radii from CERES-like aqua MODIS retrievals. Atmospheric Chemistry and Physics, 13(19), 9997–10003. 10.5194/acp-13-9997-2013

Painemal D, & Zuidema P (2011). Assessment of MODIS cloud effective radius and optical thickness retrievals over the Southeast Pacific with VOCALS-REx in situ measurements. Journal of Geophysical Research: Atmospheres, 116(D24). 10.1029/2011JD016155

Park RJ, Jacob DJ, & Logan JA (2007). Fire and biofuel contributions to annual mean aerosol mass concentrations in the United States. Atmospheric Environment, 41(35), 7389–7400. 10.1016/j.atmosenv.2007.05.061

Peltier RE, Sullivan AP, Weber RJ, Brock CA, Wollny AG, Holloway JS, et al. (2007). Fine aerosol bulk composition measured on WP-3D research aircraft in vicinity of the Northeastern United States—Results from NEAQS. Atmospheric Chemistry and Physics, 7(12), 3231–3247. 10.5194/acp-7-3231-2007

Penner JE, Dickinson RE, & Oneill CA (1992). Effects of aerosol from biomass burning on the global radiation budget. Science, 256(5062), 1432–1434. 10.1126/science.256.5062.1432 [PubMed: 17791612]

Platt WJ, Orzell SL, & Slocum MG (2015). Seasonality of fire weather strongly influences fire regimes in South Florida Savanna-Grassland Landscapes. PLOS One, 10(1), e0116952. 10.1371/journal.pone.0116952 [PubMed: 25574667]

Pósfai M, Simonics R, Li J, Hobbs PV, & Buseck PR (2003). Individual aerosol particles from biomass burning in Southern Africa: 1. Compositions and size distributions of carbonaceous particles. Journal of Geophysical Research: Atmospheres, 108(D13). 10.1029/2002JD002291

Pratt KA, Murphy SM, Subramanian R, DeMott PJ, Kok GL, Campos T, et al. (2011). Flight-based chemical characterization of biomass burning aerosols within two prescribed burn smoke plumes. Atmospheric Chemistry and Physics, 11(24), 12549–12565. 10.5194/acp-11-12549-2011

Prichard SJ, O'Neill SM, Eagle P, Andreu AG, Drye B, Dubowy J, et al. (2020). Wildland fire emission factors in North America: Synthesis of existing data, measurement needs and management applications. International Journal of Wildland Fire, 29(2), 132–147. 10.1071/wf19066

Reid JS, Koppmann R, Eck TF, & Eleuterio DP (2005). A review of biomass burning emissions—Part II: Intensive physical properties of biomass burning particles. Atmospheric Chemistry and Physics, 5, 799–825. 10.5194/acp-5-799-2005

Rogers HM, Ditto JC, & Gentner DR (2020). Evidence for impacts on surface-level air quality in the northeastern US from long-distance transport of smoke from North American fires during the Long Island Sound Tropospheric Ozone Study (LISTOS) 2018. Atmospheric Chemistry and Physics, 20(2), 671–682. 10.5194/acp-20-671-2020

Rolph GD, Draxler RR, Stein AF, Taylor A, Ruminski MG, Kondragunta S, et al. (2009). Description and verification of the NOAA smoke forecasting system: The 2007 fire season. Weather and Forecasting, 24(2), 361–378. 10.1175/2008WAF2222165.1

Rolph GD, Stein A, & Stunder B (2017). Real-time environmental applications and display system: Ready. Environmental Modelling & Software, 95, 210–228. 10.1016/j.envsoft.2017.06.025

Roy A, Choi Y, Souri AH, Jeon W, Diao L, Pan S, & Westenbarger D (2018). Effects of biomass burning emissions on air quality over the continental USA: A three-year comprehensive evaluation accounting for sensitivities due to boundary conditions and plume rise height. In Environmental contaminants (pp. 245–278). Springer. 10.1007/978-981-10-7332-8_12

Sapkota A, Symons JM, Kleissl J, Wang L, Parlange MB, Ondov J, et al. (2005). Impact of the 2002 Canadian Forest Fires on particulate matter air quality in Baltimore City. Environmental Science & Technology, 39(1), 24–32. 10.1021/es035311z [PubMed: 15667071]

Schlosser JS, Braun RA, Bradley T, Dadashazar H, MacDonald AB, Aldhaif AA, et al. (2017). Analysis of aerosol composition data for western United States wildfires between 2005 and 2015: Dust emissions, chloride depletion, and most enhanced aerosol constituents. Journal of Geophysical Research: Atmospheres, 122(16), 8951–8966. 10.1002/2017JD026547

Schmidt KM (2002). Development of coarse-scale spatial data for wildland fire and fuel management. US Department of Agriculture, Forest Service, Rocky Mountain Research Station.

Schroder JC, Campuzano-Jost P, Day DA, Shah V, Larson K, Sommers JM, et al. (2018). Sources and secondary production of organic aerosols in the northeastern United States during WINTER. Journal of Geophysical Research: Atmospheres, 123(14), 7771–7796. 10.1029/2018JD028475

Sevimoğlu O, & Rogge WF (2019). Seasonal variations of PM_{10}—Trace elements, PAHs and Levoglucosan: Rural sugarcane growing area versus coastal urban area in southeastern Florida, USA. Part II: Elemental concentrations. Particuology, 46, 99–108. 10.1016/j.partic.2019.05.001

Solomon PA, Crumpler D, Flanagan JB, Jayanty RKM, Rickman EE, & McDade CE (2014). US National $PM_{2.5}$ chemical speciation monitoring networks-CSN and IMPROVE: Description of networks. Journal of the Air & Waste Management Association, 64(12), 1410–1438. 10.1080/10962247.2014.956904 [PubMed: 25562937]

Sorooshian A, Anderson B, Bauer SE, Braun RA, Cairns B, Crosbie E, et al. (2019). Aerosol-cloud-meteorology interaction airborne field investigations: Using lessons learned from the US West Coast in the design of activate off the US East Coast. Bulletin of the American Meteorological Society, 100(8), 1511–1528. 10.1175/Bams-D-18-0100.1 [PubMed: 33204036]

Sorooshian A, Corral AF, Braun RA, Cairns B, Crosbie E, Ferrare R, et al. (2020). Atmospheric research over the Western North Atlantic Ocean Region and North American East Coast: A review of past work and challenges ahead. Journal of Geophysical Research: Atmospheres, 125, 1–54. 10.1029/2019jd031626

Stein AF, Draxler RR, Rolph GD, Stunder BJB, Cohen MD, & Ngan F (2015). NOAA's HYSPLIT atmospheric transport and dispersion modeling system. Bulletin of the American Meteorological Society, 96(12), 2059–2077. 10.1175/BAMS-D-14-00110.1

Sullivan AP, Guo H, Schroder JC, Campuzano-Jost P, Jimenez JL, Campos T, et al. (2019). Biomass burning markers and residential burning in the WINTER aircraft campaign. Journal of Geophysical Research: Atmospheres, 124(3), 1846–1861. 10.1029/2017JD028153

Sullivan AP, Peltier RE, Brock CA, de Gouw JA, Holloway JS, Warneke C, et al. (2006). Airborne measurements of carbonaceous aerosol soluble in water over northeastern United States: Method development and an investigation into water-soluble organic carbon sources. Journal of Geophysical Research: Atmospheres, 111(23), 1–14. 10.1029/2006jd007072 [PubMed: 20411040]

Tackett JL, Winker DM, Getzewich BJ, Vaughan MA, Young SA, & Kar J (2018). CALIPSO lidar level 3 aerosol profile product: Version 3 algorithm design. Atmospheric Measurement Techniques, 11(7), 4129–4152. 10.5194/amt-11-4129-2018 [PubMed: 33510819]

Taubman BF, Marufu LT, Vant-Hull BL, Piety CA, Doddridge BG, Dickerson RR, & Li ZQ (2004). Smoke over haze: Aircraft observations of chemical and optical properties and the effects on heating rates and stability. Journal of Geophysical Research, 109(D2). 10.1029/2003jd003898

Thornhill KL, Chen G, Dibb J, Jordan CE, Omar A, Winstead EL, et al. (2008). The impact of local sources and long-range transport on aerosol properties over the northeast US region during INTEX-NA. Journal of Geophysical Research: Atmospheres, 113(D8). 10.1029/2007JD008666

Trepte QZ, Minnis P, Sun-Mack S, Yost CR, Chen Y, Jin Z, et al. (2019). Global cloud detection for ceres edition 4 using terra and aqua modis data. IEEE Transactions on Geoscience and Remote Sensing, 57(11), 9410–9449. 10.1109/TGRS.2019.2926620

Twomey S (1977). Influence of pollution on shortwave albedo of clouds. Journal of the Atmospheric Sciences, 34(7), 1149–1152. 10.1175/1520-0469(1977)034<1149:Tiopot>2.0.Co;2

U.S. Environmental Protection Agency. (2014). National emissions inventory.

Val Martin M, Heald CL, Ford B, Prenni AJ, & Wiedinmyer C (2013). A decadal satellite analysis of the origins and impacts of smoke in Colorado. Atmospheric Chemistry and Physics, 13(15), 7429–7439. 10.5194/acp-13-7429-2013

Val Martín M, Honrath RE, Owen RC, Pfister G, Fialho P, & Barata F (2006). Significant enhancements of nitrogen oxides, black carbon, and ozone in the North Atlantic lower free troposphere resulting from North American boreal wildfires. Journal of Geophysical Research, 111(23), 1–17. 10.1029/2006JD007530 [PubMed: 20411040]

Vaughan MA, Powell KA, Kuehn RE, Young SA, Winker DM, Hostetler CA, et al. (2009). Fully automated detection of cloud and aerosol layers in the CALIPSO Lidar measurements. Journal of Atmospheric and Oceanic Technology, 26(10), 2034–2050. 10.1175/2009JTECHA1228.1

Wang J, Christopher SA, Nair US, Reid JS, Prins EM, Szykman J, & Hand JL (2006). Mesoscale modeling of Central American smoke transport to the United States: 1. “Top-down” assessment of emission strength and diurnal variation impacts. Journal of Geophysical Research: Atmospheres, 111(D5). 10.1029/2005JD006416

Warneke C, de Gouw JA, Stohl A, Cooper OR, Goldan PD, Kuster WC, et al. (2006). Biomass burning and anthropogenic sources of CO over New England in the summer 2004. Journal of Geophysical Research: Atmospheres, 111(D23). 10.1029/2005JD006878

Washenfelder RA, Attwood AR, Brock CA, Guo H, Xu L, Weber RJ, et al. (2015). Biomass burning dominates brown carbon absorption in the rural southeastern United States. Geophysical Research Letters, 42(2), 653–664. 10.1002/2014GL062444

Westerling AL, & Swetnam TW (2003). Interannual to decadal drought and wildfire in the Western United States. Eos, 84(49), 545. 10.1029/2003EO490001

Winker DM, Vaughan MA, Omar A, Hu Y, Powell KA, Liu Z, et al. (2009). Overview of the CALIPSO mission and CALIOP data processing algorithms. Journal of Atmospheric and Oceanic Technology, 26(11), 2310–2323. 10.1175/2009JTECHA1281.1

Wotawa G, & Trainer M (2000). The influence of Canadian forest fires on pollutant concentrations in the United States. Science, 288(5464), 324–328. 10.1126/science.288.5464.324 [PubMed: 10764643]

Wu YH, Arapi A, Huang J, Gross B, & Moshary F (2018). Intra-continental wildfire smoke transport and impact on local air quality observed by ground-based and satellite remote sensing in New York City. Atmospheric Environment, 187, 266–281. 10.1016/j.atmosenv.2018.06.006

Yokelson RJ, Crounse JD, DeCarlo PF, Karl T, Urbanski S, Atlas E, et al. (2009). Emissions from biomass burning in the Yucatan. Atmospheric Chemistry and Physics, 9(15), 5785–5812. 10.5194/acp-9-5785-2009

Zhang B, Owen RC, Perlinger JA, Helmig D, Val Martín M, Kramer L, et al. (2017). Ten-year chemical signatures associated with long-range transport observed in the free troposphere over the central North Atlantic. Elementa: Science of the Anthropocene, 5(0), 8. 10.1525/elementa.194

Zhang Z, & Platnick S (2011). An assessment of differences between cloud effective particle radius retrievals for marine water clouds from three modis spectral bands. Journal of Geophysical Research, 116(D20). 10.1029/2011JD016216

References From the Supporting Information

AIRS Science Team/Joao Teixeira. (2013). AIRS/Aqua L2 standard physical retrieval (AIRS-only) V006. Goddard Earth Sciences Data and Information Services Center (GES DISC). 10.5067/Aqua/AIRS/DATA202

Bond TC, Streets DG, Yarber KF, Nelson SM, Woo JH, & Klimont Z (2004). A technology-based global inventory of black and organic carbon emissions from combustion. Journal of Geophysical Research: Atmospheres, 109(D14). 10.1029/2003JD003697

Bosilovich MG, Lucchesi R, & Suarez M (2016). MERRA-2: File specification. GMAO Office Note No. 9 (Version 1.1) (p. 73). Global Modeling and Assimilation Office, NASA Goddard Space Flight Center Greenbelt. 10.5067/KLICLTZ8EM9D

Buchard V, Randles CA, da Silva AM, Darmenov A, Colarco PR, Govindaraju R, et al. (2017). The MERRA-2 aerosol reanalysis, 1980 onward. Part II: Evaluation and case studies. Journal of Climate, 30(17), 6851–6872. 10.1175/JCLI-D-16-0613.1ssss [PubMed: 32908329]

Chin M, Ginoux P, Kinne S, Torres O, Holben BN, Duncan BN, et al. (2002). Tropospheric aerosol optical thickness from the GOCART model and comparisons with satellite and Sun photometer measurements. Journal of the Atmospheric Sciences, 59(3), 461–483. 10.1175/1520-0469(2002)059<0461:TAOTFT>2.0.CO;2

Drury E, Jacob DJ, Spurr RJD, Wang J, Shinozuka Y, Anderson BE, et al. (2010). Synthesis of satellite (MODIS), aircraft (ICARTT), and surface (IMPROVE, EPA-AQS, AERONET) aerosol observations over eastern North America to improve MODIS aerosol retrievals and constrain surface aerosol concentrations and sources. Journal of Geophysical Research Atmospheres, 115(14), 1–17. 10.1029/2009JD012629

Goldstein AH, Koven CD, Heald CL, & Fung IY (2009). Biogenic carbon and anthropogenic pollutants combine to form a cooling haze over the southeastern United States. Proceedings of the National Academy of Sciences of the United States of America, 106(22), 8835–8840. 10.1073/pnas.0904128106 [PubMed: 19451635]

Huang K, Fu JS, Hsu NC, Gao Y, Dong X, Tsay SC, & Lam YF (2013). Impact assessment of biomass burning on air quality in Southeast and East Asia during BASE-ASIA. Atmospheric Environment, 78, 291–302. 10.1016/j.atmosenv.2012.03.048

Molod A, Takacs L, Suarez M, & Bacmeister J (2015). Development of the GEOS-5 atmospheric general circulation model: Evolution from MERRA to MERRA2. Geoscientific Model Development, 8(5), 1339–1356. 10.5194/gmd-8-1339-2015

Olsen ET, Fetzer E, Hulley G, Manning E, Blaisdell J, Iredell L, & Maddy E (2013). AIRS/AMSU/HSB version 6 level 2 product user guide: NASA-JPL Tech Rep.

Randles CA, da Silva AM, Buchard V, Colarco PR, Darmenov A, Govindaraju R, et al. (2017). The MERRA-2 aerosol reanalysis, 1980 onward. Part I: System description and data assimilation evaluation. Journal of Climate, 30(17), 6823–6850. 10.1175/JCLI-D-16-0609.1 [PubMed: 29576684]

Shikwambana L (2019). Long-term observation of global black carbon, organic carbon and smoke using CALIPSO and MERRA-2 data. Remote Sensing Letters, 10(4), 373–380. 10.1080/2150704X.2018.1557789

Shikwambana L, & Sivakumar V (2018). Global distribution of aerosol optical depth in 2015 using CALIPSO level 3 data. Journal of Atmospheric and Solar-Terrestrial Physics, 173, 150–159. 10.1016/j.jastp.2018.04.003

Sitnov SA, Mokhov II, & Likhosherstova AA (2020). Exploring large-scale black-carbon air pollution over Northern Eurasia in summer 2016 using MERRA-2 reanalysis data. Atmospheric Research, 235, 104763. 10.1016/j.atmosres.2019.104763

Torres O, Ahn C, & Chen Z (2013). Improvements to the OMI near-UV aerosol algorithm using A-Train CALIOP and AIRS observations. Atmospheric Measurement Techniques, 6(11), 3257–3270. 10.5194/amt-6-3257-2013

Torres O, Bhartia P, Ahn C, & Leonard P, (2018). OMI/Aura near UV aerosol index, optical depth and single scattering albedo 1-Orbit L2 13 × 24 km, NASA Goddard Space Flight Center. Goddard

Earth Sciences Data and Information Services Center (GES DISC). 10.5067/MEASURES/AER/DATA203

Key Points:

- Biomass burning (BB) particles over U.S. East Coast and Bermuda are common year-round with varying sources and at altitudes impacting clouds
- Smoke-cloud interactions are likely based on higher cloud drop number concentration and lower drop effective radius on BB days
- A significant reduction in cloud liquid water path was noted on days with enhanced columnar and surface smoke over the study region

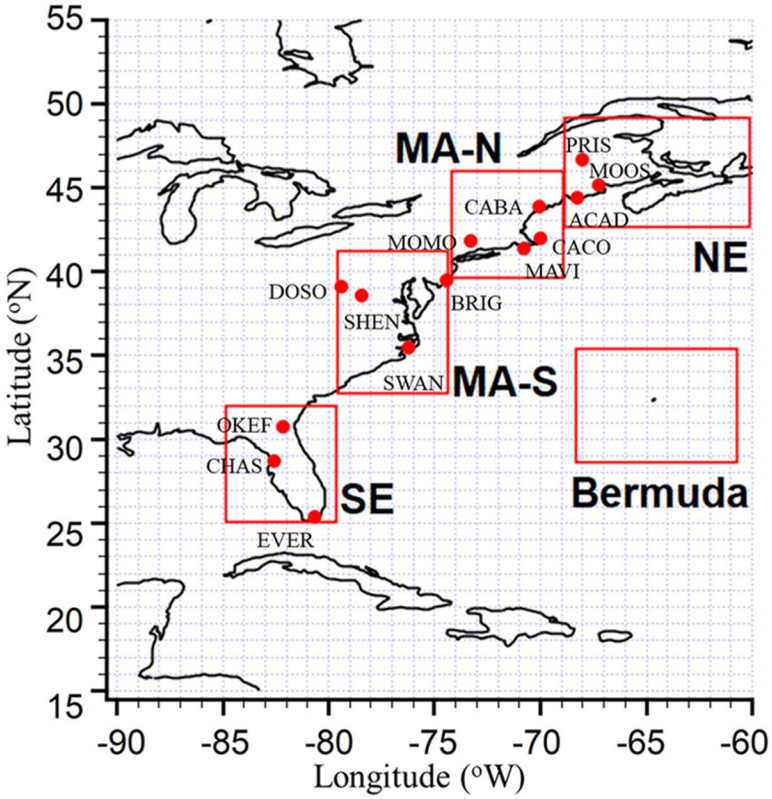

Figure 1.

A map of the study region showing the five sub-domains of interest in red boxes: NE, northeast U.S.; MA-N, northern mid-Atlantic states; MA-S, southern mid-Atlantic states; SE, southeast U.S. Red dots denote IMPROVE stations from which data were used.

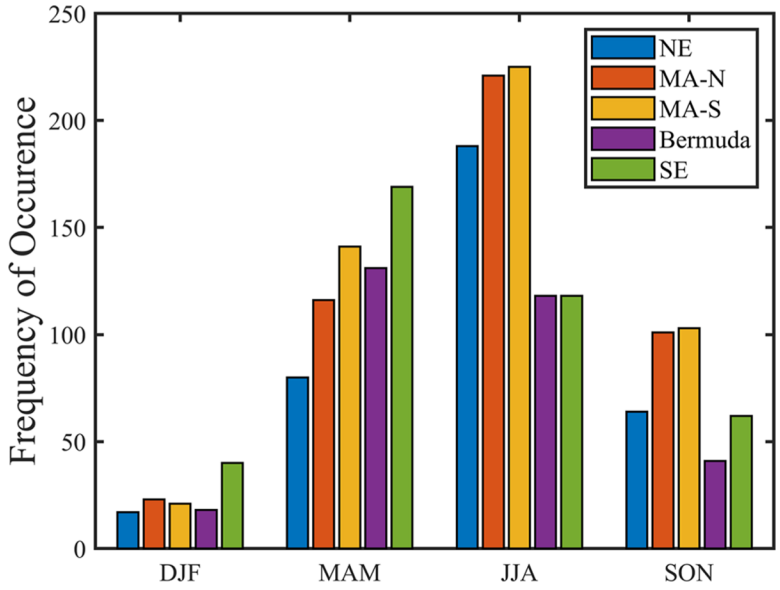

Figure 2.

Number of BB days in each sub-domain for December–February (DJF), March–May (MAM), June–August (JJA), and September–November (SON). This analysis applies to 1 January 2005 through 31 December 2018. Total number of BB days including all seasons for the studied time period are as follows: NE = 349; MA-N = 461; MA-S = 490; Bermuda = 308; SE = 389.

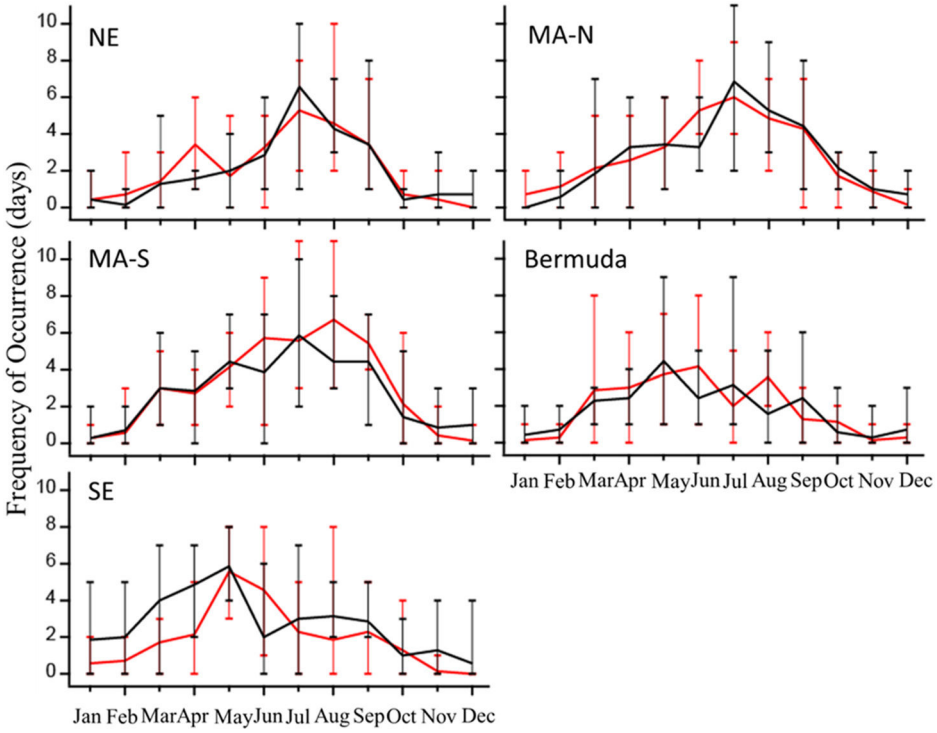

Figure 3.

Mean-annual frequency of occurrence of BB days in each month for 2005–2011 (red) and 2012–2018 (black) over each sub-domain. The ends of the whiskers denote minimum and maximum values.

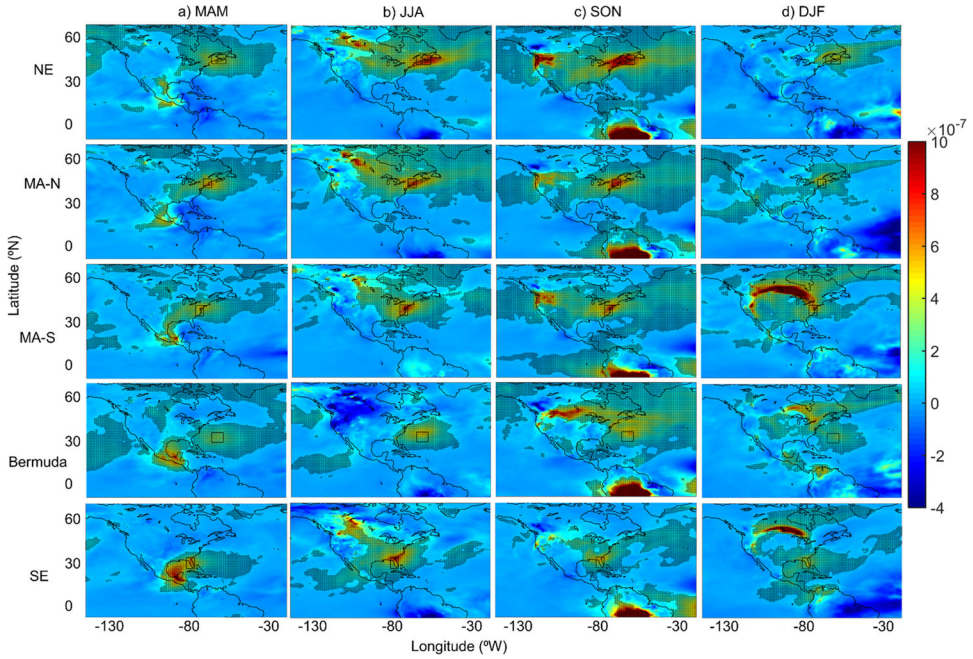

Figure 4.

Spatial maps of black carbon column density anomaly (kg m^{-2}) for each respective sub-domain for (a) March–May (MAM), (b) June–August (JJA), (c) September–November (SON), and (d) December–February (DJF), computed as the difference between the mean MERRA-2 BC value on BB days and the mean value of all days in each respective set of months. Hashed areas denote grids where the anomaly value is statistically significant with 95% confidence based on the Student's t-test. The black box denotes the sub-domain that the analysis was conducted for in each composite map.

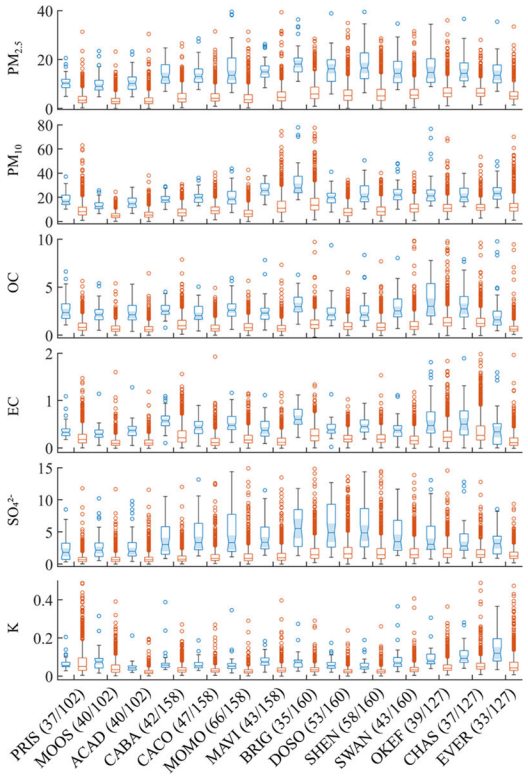

Figure 5.

The average mass concentrations of IMPROVE species (μg m^{-3}) for BB-impacted days (in blue) with anomalously high deseasonalized $PM_{2.5}$ levels (>90th percentile) (called BB + $PM_{2.5}$) and non-BB days (in red) with available IMPROVE data for the study period (January 1, 2005 through December 31, 2018). Numbers in parenthesis after each IMPROVE site label represents: # of days with available IMPROVE data that qualified as a BB day and also exhibited anomalously high deseasonalized $PM_{2.5}$ levels (>90th percentile)/# of days with available IMPROVE data that qualified as a BB day. For each box-plot, 25th percentile, the median, and 75th percentile are denoted with the bottom, middle, and top lines of the box, respectively. Extreme values are presented as colored circles, based on a distance of 1.5 × interquartile range from the top of each box. Maximum and minimum values are depicted by whiskers, not including the extreme values. Boxes with notches and shaded regions that do not overlap have statistically different medians with 95% confidence. Seasonal results are in Tables S7–S10 in Supporting Information S1.

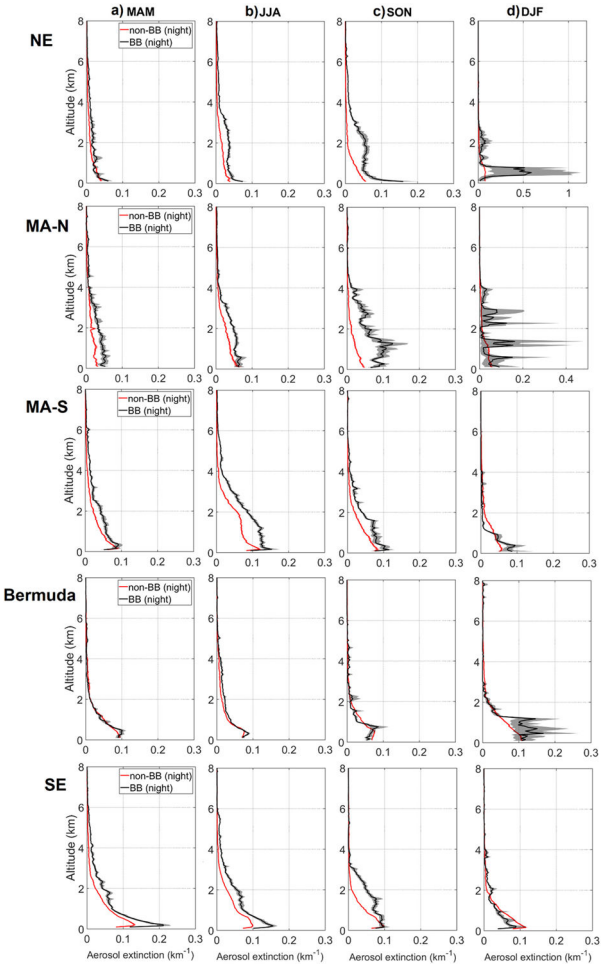

Figure 6.

Mean aerosol extinction coefficient at 532 nm from CALIOP over each sub-domain for June 2006 – December 2018 for BB and non-BB days for nighttime observations. Shading represents the 95% confidence interval of the mean profile estimated based on bootstrapping (n = 10,000). Analogous results for daytime conditions are in Figure S7 in Supporting Information S1.

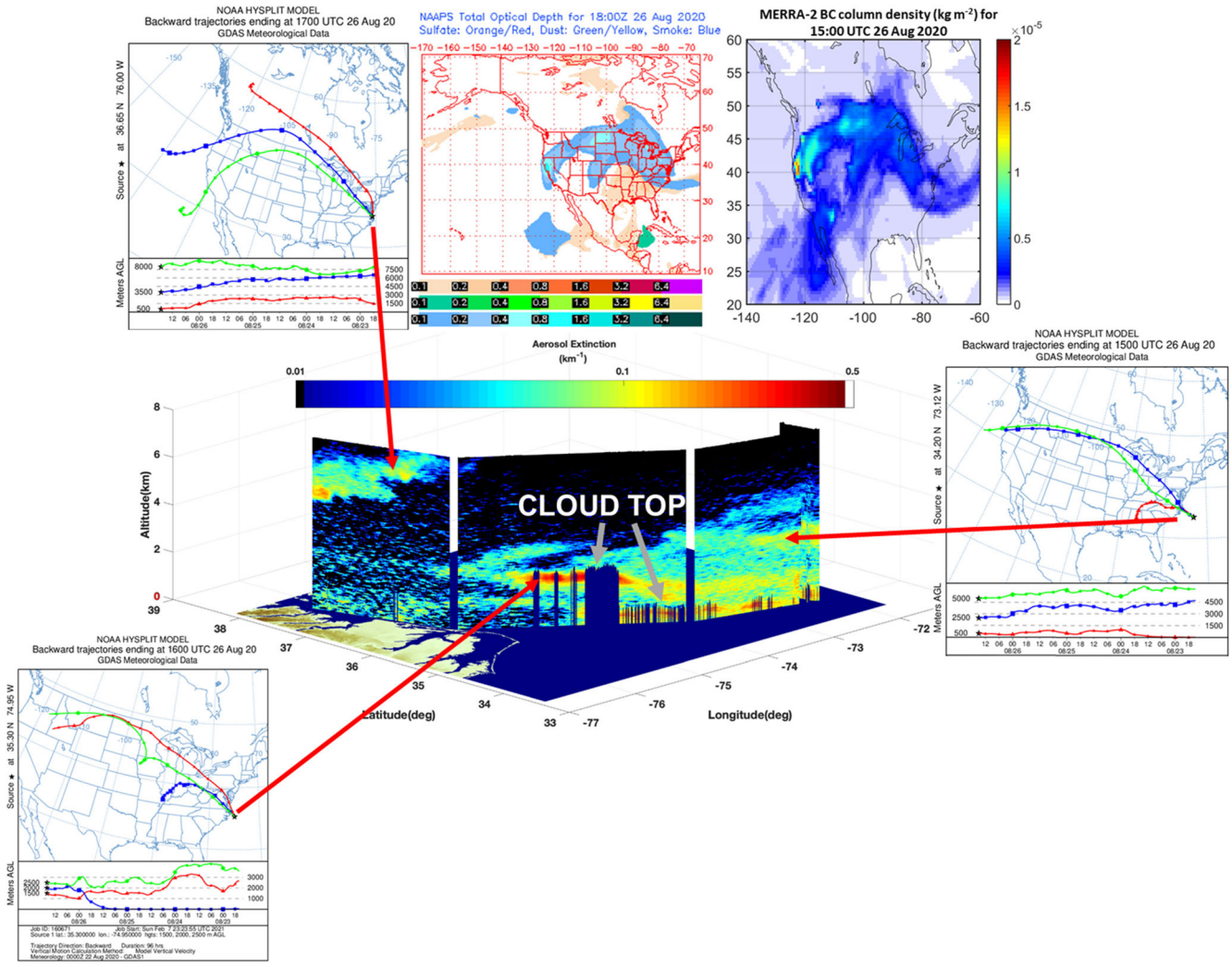

Figure 7.

HSRL-2 curtain of aerosol extinction (532 nm) during ACTIVATE's Research Flight 28 on 26 August 2020. Shown in the peripheral panels are spatial maps of NAAPS speciated optical depths and MERRA-2 BC column density, and representative NOAA HYSPLIT back-trajectories from points during the flight. Gray arrows point to two subsets of cloud tops with higher clouds to the left and lower clouds in the boundary layer to the right.

Table 1

Seasonal (and "All" for All Data) Mean Values of Liquid Cloud Parameters From CERES-MODIS Edition 4 Single Scanning Footprint (SSF) Data for Non-BB and BB Days

		Cloud fraction (%)		LWP (g m^{-2})		Cloud N_d (cm^{-3})		Cloud r_e (μm)	
		Non-BB	**BB**	**Non-BB**	**BB**	**Non-BB**	**BB**	**Non-BB**	**BB**
DJF	NE	50	56	135	148	**69**	**111**	**13.9**	**12.6**
	MA-N	**48**	**57**	130	153	92	104	13.2	12.5
	MA-S	45	40	118	87	104	123	11.8	11.5
	SE	42	37	60	64	**80**	**110**	11.5	10.9
	Bermuda	51	46	**65**	**41**	37	44	14.0	12.5
MAM	NE	48	45	118	129	**81**	**96**	13.1	12.7
	MA-N	47	45	112	141	**105**	**133**	11.7	11.3
	MA-S	44	45	90	101	111	124	10.9	10.7
	SE	40	39	43	51	78	86	11.5	11.7
	Bermuda	46	45	48	45	**39**	**49**	**13.5**	**12.8**
JJA	NE	**45**	**40**	**94**	**67**	86	79	11.6	11.6
	MA-N	**43**	**39**	89	71	**97**	**82**	**10.8**	**11.2**
	MA-S	40	38	**57**	**44**	**85**	**72**	10.6	10.9
	SE	35	31	56	43	58	61	12.3	12.1
	Bermuda	38	39	32	31	**34**	**51**	13.6	12.5
SON	NE	49	51	121	90	**73**	**112**	**12.8**	**11.1**
	MA-N	48	44	121	87	94	103	11.6	11.0
	MA-S	46	42	**104**	**70**	90	104	11.3	10.8
	SE	**40**	**33**	55	37	62	70	12.5	11.6
	Bermuda	46	47	54	36	29	19	14.3	15.4
All	NE	**48**	**44**	**120**	**93**	**76**	**91**	**13.0**	**11.9**
	MA-N	**47**	**44**	118	108	**96**	**107**	**12.1**	**11.3**
	MA-S	44	42	**99**	**75**	99	104	**11.3**	**10.8**
	SE	**41**	**38**	54	51	**74**	**89**	11.8	11.5
	Bermuda	**48**	**45**	**57**	**42**	**36**	**48**	**13.9**	**12.8**

Note. Numbers in bold denote a statistical significance between the pair of values at the 95% confidence level based on the Student's *t*-test. This analysis applies to January 1, 2005 through December 31, 2018, and applies to low-level liquid clouds when cloud fraction exceeds 30%, as described in Section 2.6.